Transferable Intermolecular Potentials for Carboxylic Acids and Their Phase Behavior

Amir Vahid and J. Richard Elliott
Chemical and Biomolecular Engineering Dept., The University of Akron, Akron, OH 44325

DOI 10.1002/aic.11966
Published online August 24, 2009 in Wiley InterScience (www.interscience.wiley.com).

Transferable step potentials are characterized for 39 carboxylic acids. The reference potential is treated with discontinuous molecular dynamics, including detailed molecular structure. Thermodynamic perturbation theory is used to interpret the simulation results and to provide an efficient basis for molecular modeling and characterization of the attractive forces. Four steps are used for representation of the attractive forces with only the first and last steps varied independently. The two middle steps are interpolated such that each site type is characterized by three parameters: the diameter, σ, the depth of the inner well, ε_1, and the depth of the outer well, ε_4. The depths of the attractive wells are optimized to fit experimental vapor pressure and liquid density data. Generally, the vapor pressure is correlated to an overall 43% average absolute deviation (% AAD) and the liquid density to 5% AAD. The deviations tend to be largest for the higher molecular weight acids. These deviations are larger than the errors previously encountered in characterizing organic compounds, but carboxylic acids present exceptional challenges owing to their peculiar dimerization behavior. Simultaneous correlation of vapor pressure, vapor compressibility factor, and phase equilibria of water + carboxylic acids place several constraints on the nature of the potential model, with the parameters of the present model representing a reasonable tradeoff. In other words, our model represents minimal deviations for vapor pressure, vapor compressibility factor, and phase equilibria of all acids simultaneously while varying the parameters σ, ε_1, ε_4, ε^{CC}(dimerizing site bonding energy), ε^{AD}(acceptor-donor bonding energy), and K^{HB}(hydrogen bonding volume) for the acid O= and OH site types. The present model is characterized by one acceptor and one dimerizing site on the carbonyl oxygen and one acceptor and one donor site on the hydroxyl oxygen. The acceptor and donor are capable of interacting with water while the dimerizing site is not. With this model, the saturated vapor compressibility factor of acids with seven or fewer carbons is near 0.5 while higher carbon ratios lead to a compressibility factor approaching 1.0. To compensate for the high vapor pressure deviations of the transferable potential model, a correction is introduced to customize the molecule-molecule self interaction energy. This adaptation results in deviations of 3.1% for vapor pressure of the pure acid database. To validate the behavior of the model for carboxylic acids in mixtures, 33 binary solutions were considered. Acids in this database ranged from formic to hexadecanoic. The average absolute deviation in bubble pressure for

Additional Supporting Information may be found in the online version of this article.

Correspondence concerning this article should be addressed to J. R. Elliott at dickelliott@uakron.edu

aqueous acid systems is 4.4%, 10.5% for acid + acid systems, and 4.7% for acid + n-alkane systems without a customized interaction correction. When applying the correction, deviations were 2.4% for aqueous systems, 2% for acid systems, and 2.8% for acid + n-alkane systems. © 2009 American Institute of Chemical Engineers *AIChE J*, 56: 485–505, 2010

Keywords: molecular simulation, vapor pressure, compressibility factor, phase equilibria

Introduction

Carboxylic acids have important roles in both the chemical and pharmaceutical industries. For example, aspirin is a multifunctional type of carboxylic acid that is used for medical purposes. Also, carboxylic acids are important constituents of biofuels and are encountered in biochemical applications. For instance, lactic acid is used in producing renewable plastics.[1] For all these applications, it would be desirable to have a comprehensive model of the thermodynamic properties of acids, to optimize their production and efficacy. Unfortunately, acids form peculiar complexes that make it difficult to formulate such a model.

Complexes are the results of specific chemical forces that are acting between molecules. Isolation of the complexes is impossible but their existence has been proved through spectroscopic observations. Hydrogen bonding and Lewis acid/base interactions are two examples of this type of behavior.[2,3] The dimerization of acetic acid is a classic example of association, in which case complexation occurs between molecules of the same component. The peculiar feature of association in carboxylic acids is that two hydrogen bonds usually form simultaneously, resulting in a stable ring with hydroxyl sites bound to carbonyl oxygens. The O—H—O bond angle is nearly linear which means that the carboxylic acid structure is close to a six-sided ring, not an eight-sided ring, introducing little ring strain and stabilizing the dimer.[4] This makes the dimerization quite strong but terminates the chain reaction such that higher oligomers are few. If this was the only possibility, then a simple model would be feasible in which acids can only complex with other acids.[5] This model could be represented by a special bonding site in which the hydroxyl and carbonyl are lumped together. But such a model would not explain the favorable interactions between acids and water, or alcohols. Another possibility is to assume that acid bonding sites can interact freely with both acids and other bonding sites.[6–10] Such a model explains some behaviors accurately, but falls short in modeling others, as discussed below. Many other characterizations have been considered with varying degrees of success, as described in the background section. It is also worth mentioning that there are multiple crystalline polymorphs for some of carboxylic acid crystals like cinchomeronic[11] and tetrolic acids.[12] Also, a quite large number of carboxylic acids have a chain motif instead of the dimer motif as mentioned by Gavezzotti et al.[12] Note that considering these solid systems is beyond the scope of the present work.

One of the most powerful theories of complexation is Wertheim's[13] perturbation theory. This theory derives from a rigorous analysis of cluster diagram expansions and a renormalization recognizing that the change in fluid structure is small even when the energy of the complex is large. In Wertheim's theory, the bonding is represented by small attractive sites located near the surface of a large repulsive site. This arrangement enforces the linearity of the bonding angle and controls the entropy of bonding through the size of the bonding site. The accuracy of this theory has been demonstrated using molecular simulations.[14,15] Wertheim's theory has been adapted for several models of complexation, including ESD,[16] SAFT,[16,17] PC-SAFT,[16,18–20] and CPA.[18,21] Recently, we have been adapting Wertheim's theory to characterize complexation in a detailed molecular model of step potentials for equilibria and discontinuous molecular dynamics (SPEADMD),[22] the subject of the present work. In SPEADMD, a molecular simulation of the repulsive core of the molecule is conducted, including the details of the chains, branching, rings, and steric hindrance. This requires roughly 8 h per compound to obtain the entire $P(V,T)$ characterization. The perturbations are then applied through the theories that have been proved accurate, Wertheim's theory for complexes and Barker-Henderson theory[23] for the disperse attractive interactions.

In the case where a six-membered ring is formed, Wertheim's theory has limitations. Wertheim's theory does not directly distinguish the locations of bonding sites on molecules. Simply exaggerating the hydroxyl-carbonyl interaction would not recognize the favorability of ring closure at low density. The ring closure is key to forming dimers rather than chains. Sear and Jackson[24,25] have explored the fundamentals of ring formation within Wertheim's theory, but no practical model for acids has resulted.

In this work, we develop a model that recognizes strong dimerization but allows for relatively weak acid chain oligomers. In this way, the strong dimerization accounts for the speciation of ring dimers at all densities while the remaining sites account for the rare chain dimers, trimers, etc. The chain sites also permit interaction with water and alcohols. By characterizing chain site association as a weak interaction and chain site solvation with water and alcohols as a strong interaction, we hope to achieve a reasonable representation of the speciation at all conditions of density and composition. The flaw in this model is the failure to recognize that a closed ring and an acid chain should not exist simultaneously when counting bonds rigorously. Thus, for example, we would expect the model to overestimate acid dimerization in dilute aqueous solutions. On the other hand, the interactions in acids may not conform to such strict bond counting anyway. So treating the interactions in this manner is worth considering. After reviewing the literature more extensively in the background section, we characterize association for acids ranging from C_1 to C_{19}, including the trend in vapor compressibility factor (Z_V^{sat}) as

well as vapor pressure. The section on mixtures presents the characterization of solvation interactions using a preliminary model of water. We find systematic deviations in the properties when applying transferable potential models, but the qualitative trend is correct over a broad range of conditions and compounds, and quantitative results can be easily obtained by customizing the dispersion energy for a particular compound. In this article, transferability means that the optimized force field parameter for smaller carboxylic acids can be applied to higher ones.

The scope of this study is limited to thermodynamic properties. Transport properties will be studied in future works. In general, SPEADMD yields acceptable correlations for transport properties of the liquid phase for nonassociating species. Extensions to acids must account for the lifetime of the hydrogen bond and the decay of the autocorrelation function. Analyzing these effects would require explicit simulation of the full potential because no transport theory is available comparable to the thermodynamic perturbation theory. Nevertheless, it is unlikely that the current potential model would be optimal for transport properties and such a multiproperty analysis would undoubtedly shed light on more details of the potential model.

Background on Hydrogen Bonding in Carboxylic Acids

Numerous studies of complexation in acids have contributed to our understanding of association and solvation in acid systems. Tsonopoulos and Prausnitz[26] analyzed the vapor phase association of water and carboxylic acids. In their work, the effect of dimerization and trimerization of carboxylic acids in the vapor phase was considered and the solvation between water and carboxylic acid was asserted to be very weak. This assertion was validated by Wolbach and Sandler,[27–29] with quantum mechanical ab initio calculations based on the Gibbs energy of formation of acid + acid and acid + water dimerization. It was observed that the acid + acid dimerization is about 100 times stronger than acid + water solvation. Nevertheless, the Gibbs free energy was negative for both cases. Later, Colominas et al.[30] implemented density functional theory (DFT) and ab initio modeling to find that the free energy of dimerization of carboxylic acid in the gas phase varies from -2 to -4 kcal/mol while the dimerization free energy in (1 M) water was clearly positive ($\sim$4–5 kcal/mol).

Modeling of carboxylic acid systems with SAFT style equations of state was initiated by Huang and Radosz.[17,31] They obtained reasonable values for vapor pressure deviations without using transferable parameters. Kontogeorgis and coworkers[6–9,32] have tried to characterize an associated model for pure carboxylic acid along with a solvation term for mixtures like the acetic acid + water system. They characterized the correct trends but their results have higher errors in VLE and LLE than Grenzheuser and Gmehling.[5] Moreover, their association model varies with the system of interest and they did not apply their carboxylic acid site type, i.e., "1A," for all systems containing carboxylic acids. Recently, a comprehensive study on phase equilibrium of mixtures containing acetic acid has been performed by Muro-Suñé et al.[33] They considered systems including gas solubilities, solvation systems with water and alcohols, and polar compounds like acetone and esters. Although their nontransferable model gives excellent results for a large variety of systems using a simple 1A association scheme for acetic acid, it fails to predict the pinch point in mixtures of acetic acid + water at rich water concentrations. Furthermore, the peculiar behavior of Z_V^{sat} has not been mentioned in their work. The best SAFT and CPA family model for the water + acetic acid mixture has been proposed by Perakis et al.[34] This work demonstrated that the 3B (three site types) model of water provided the most accurate correlation of VLE and LLE. Perakis et al. also observed that the intermolecular interactions between water and acetic acid lead to strong solvation, overcoming the association of the water molecules. There are two notable limitations in the work of Perakis et al., however. The first one is that they have only reported their model results for acetic acid without mentioning the behavior of Z_V^{sat}. The second shortcoming is again related to the lack of a transferable approach for model parameterization from smaller acids to larger ones. In this work, we used a 4C (four hydrogen bonding site types) model for water which has two acceptor and two donor sites following Huang and Radosz.[17,31] The 4C model was reported to be the most accurate for many systems studied by Gross and Sadowski,[20,35] and we find that its accuracy for mixtures with acid systems is satisfactory.

Regarding aspects of the SPEADMD model other than the treatment of association, the SPEADMD model is based on molecular simulation of the specific molecular structure at hand, rather than a coarse grained model like tangent sphere chains. Molecular modeling has many advantages over engineering equations of state and group contribution methods. There are several related studies of acids that apply molecular modeling in detail. Kamath et al.,[36,37] Clifford et al.,[38] and Schnabel et al.[39] performed a detailed molecular simulation combined with quantum mechanics analysis for liquid and vapor density of pure carboxylic acids and also VLE of mixtures containing those acids based on soft potentials and point charged force fields such as Lennard-Jones and Trappe-UA. Their results have a relatively high error ($\sim$30% AAD) for the vapor density of carboxylic acids and they did not report acid-water solvation in their research. The SPEADMD model has been developed and tested for roughly 500 compounds comprising 35 families. These families include thiophene, fluorocarbon, alcohol, amine, aromatic, and ring compounds to name just a few examples.[40,41] However, the carboxylic acid family has presented a longstanding obstacle. With this background, we seek a molecular model with transferable potentials that captures the key features of acid phase behavior. These features should encompass the trend of Z_V^{sat} with molecular weight as well as the VLE and LLE in mixtures with acids, alkanes, alcohols, and water.

Transferable Potentials, Molecular Simulation, and Equations of State

The SPEADMD model is based on simulation of each particular molecule combined with thermodynamic perturbation theory (TPT). The molecules to be simulated are composed of interaction sites that include both repulsive and attractive

interactions, but only the repulsive interactions are simulated explicitly, as these dominate the nature of the ensemble averaged configurations. TPT is applied to expedite the simulation and optimal characterization of the attractive interactions. Numerous studies have confirmed the accuracy of TPT when compared to the rigorous simulation of the full potential model (with attractions and repulsions included).[42–44] To a reasonable approximation, the characterizations of potential energy around each interaction site are transferable from one molecule to another. For example, the potential that describes a CH_2 site in *n*-nonane can be applied to a CH_2 site in *n*-pentadecane with accuracy of roughly 10% in vapor pressure and 2% in liquid density. Simulations are conducted at 21 densities to permit accurate interpolation between state points. Noting that TPT describes the temperature dependence, the result is a complete equation of state for $P(V,T)$. By comparing the $P(V,T)$ properties for each characterization of the potential function to experimental data, an optimal set of potential models can be obtained. This methodology has been described in more detail by Elliott et al.,[45] including preliminary predictions of transport properties. The following subsections provide a brief introduction to the key relations.

Transferable potentials

The potential models applied in SPEADMD have been constructed to facilitate their implementation with TPT. Two distinct forms of TPT make important contributions, one for disperse interactions[23] and one for complexes.[13,46]

For the disperse interactions, a series of multiple steps has been found to provide satisfactory characterization of vapor pressure, density, and phase behavior. The hard repulsive core facilitates the analysis of the reference system. If a soft reference were used, then reference simulations would be necessary over a range of temperatures as well as densities. Since most applications to phase equilibria occur in the range of 300–500 K, assuming a constant reference diameter over that range is reasonable. For disperse attractions, initial efforts focused on simple 4-step potentials ranging from the site diameter, σ, to a distance of 2σ.[47,48] The steps in these potentials occur at 1.2σ, 1.5σ, 1.8σ, and 2.0σ, which we designate as a 2580 potential model. Recent work has shown that 11-step potentials ranging from σ to 3σ can be defined that mimic continuous potentials like the Lennard-Jones or Yukawa models and provide improved accuracy while reducing the number of attractive parameters to one per site type.[49] Since the 11-step potentials are relatively new and have not been extended to the complete database, the present work applies the linear 2580 model of Unlu et al.[48]

There are three parameters per site type in the linear 2580 model: the diameter, the depth of the inner well, and the depth of the outer well. The depths of the intermediate wells are linearly interpolated according to,

$$\varepsilon_{ijm} = \frac{(4-m)\varepsilon_{ij1} + (m-1)\varepsilon_{ij4}}{3} \tag{1}$$

Also, Lorentz-Berthelot combining rules were used to calculate mixed site–site interactions

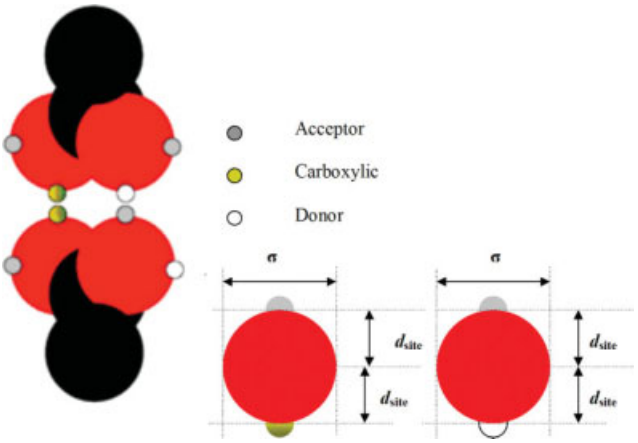

Figure 1. A blister potential model of association for carboxylic acids.

A, D, and C-sites are combined with strong association for C-sites and weak associations between A- and D-sites. [Color figure can be viewed in the online issue, which is available at www.interscience.wiley.com.]

$$\varepsilon_{ijm} = (\varepsilon_{im}\varepsilon_{jm})^{1/2}(1 - k_{ij}^{ss}) \tag{2}$$

$$\sigma_{ij} = \frac{1}{2}(\sigma_i + \sigma_j) \tag{3}$$

where k_{ij}^{ss} represents the site–site interaction parameter which corrects for deviations from this guideline. The present work assumes $k_{ij}^{ss} = 0$.

For the hydrogen bonding interactions in acids, blister potentials consistent with Wertheim's theory are applied. The Wertheim theory with its TPT characteristics is implemented for highly simplified models in which the associating species are considered with hard repulsive cores combined with a group of attractive sites. The associations are considered as off-center, square-well (SW) potentials with a well depth of ε^{HB} and well width of 0.25σ. The repulsive hard spheres cannot overlap and hence the SW potential is sufficiently short ranged that the formation of more than one bond at the locations of any given sites is forbidden due to steric incompatibility.[15,50] An illustration of the hydrogen bonding sites is given in Figure 1. Clearly, the dimer in this figure has a free donor site, whereas both donor sites should be consumed in forming a stable ring dimer. Thus, as mentioned earlier, in our model the strong dimerization accounts for ring dimers and the excess donor sites account for the chain dimers, trimers, etc. Wertheim's theory has no provision for forming a closed ring relative to a linear chain therefore our model treats these separately. Our goal is to achieve a reasonable representation of the oligomer distributions (monomer, dimer, trimer, etc.) as a function of temperature and density. We contend that a relatively narrow range of oligomer distributions is consistent with the thermodynamic observations and our model is capable of characterizing them. Once this range is characterized, other models could be conceived that reproduce it in a more sophisticated fashion. The pursuit of models that distinguish between intermolecular and intramolecular bonding and ring closure will be the subject of future research. The acceptor (A) and donor (D) sites are similar in size to those of alcohols and

amines,[48,51] but their association energy is relatively weak (2.1 kJ/mol). Sites of similar nature have been shown to provide reasonable estimates of the structures generated by point charge models like the TIP4P[52] and the TIP5P[53,54] models, lending further credibility to the fundamental basis of this approach. Note however that the effect of dipole–dipole interaction is embedded in the perturbation theory implicitly through the hydrogen bonding and dispersion terms. The carboxylic (C) sites are peculiar to acids. They have a much smaller bonding volume and a much larger bonding energy (94 kJ/mol). Note that the C-type bonding energy represents the formation of two hydrogen bonds. Even so, this value of the bonding energy is exaggerated roughly by a factor of two. The exaggeration in bonding energy is compensated by the extra small bonding volume. Combined, this description exaggerates the exothermic nature of the C-type interaction, causing the extent of association to decrease strongly with increasing temperature as evidenced by the experimental data for Z_V^{sat}. This combination was necessary to mimic the strong dimerization in the vapor phase of the smaller acids. The same estimates of bonding volume and bonding energy were transferred to all carboxylic acids in the current study. Many previous studies have treated acids individually.

A slightly different specification applies to the interaction energies of hydrogen bonding,

$$\varepsilon_{ij}^{HB} = \frac{(\varepsilon_i^{HB} + \varepsilon_j^{HB})}{2}(1 - k_{ij}^{AD,CC}) \tag{4}$$

The $k_{ij}^{AD,CC}$ in this combining rule reflects the possibility that solvation may be strong even when association is weak. This behavior was prevalent in alcohol-amine interactions.[22] This parameter is also very important in the presently proposed model. Although the A-D associations in acids are weak, their solvation with the A-D sites of water can be strong if a large negative value for k_{ij}^{AD} is applied.

Discontinuous molecular dynamic simulation

The SPEADMD model is based on discontinuous molecular dynamics (DMD).[55–58] In principle, the same potential models could be applied in Monte Carlo simulation, but then the dynamics that could shed light on transport properties would require a separate simulation. Long term, we seek a single model that can be applied consistently to all properties. The discontinuous aspect of the simulation derives from the discontinuous nature of the potential model, especially the hard core repulsions of the reference models. This necessitates that the dynamics be integrated through the scheduling of individual collisions. To maintain a consistent algorithm, a similar approach must be applied to the intramolecular interactions. An efficient algorithm for achieving this integration has been described by Rapaport.[56,59]

The computer simulations are carried out based on vibrating purely repulsive structure indicative united atom (UAM) molecular models without considering the O—C—O—H dihedral angle. Note that the intermolecular conformation of the A, D, and C sites in carboxylic acids are controlled by a repulsive potential and these sites are free to rotate with respect to each other and to O—C—O triad. The bond lengths are constrained to be near the known values, e.g., 0.154 nm for a C—C single bond, and bond angles restrained by comparable vibrating wells. The depths of the wells and the diameters are given in Table 1. Branches and rings are added directly to the potentials based on the molecular structure and specified by the bonded potential defined below

$$u_{ij}^{bonded} = \begin{cases} \infty & r < L_{12} - \delta_{12} \\ 0 & L_{12} - \delta_{12} \le r < L_{12} + \delta_{12} \\ \infty & L_{12} + \delta_{12} \le r < L_{13} - \delta_{13} \\ 0 & L_{13} - \delta_{13} \le r < L_{12} + \delta_{12} \\ \infty & L_{13} + \delta_{13} \le r < \sigma_{intra} \\ 0 & \sigma_{intra} \le r \end{cases} \quad u_{ij}^{non-bonded}$$

$$= u_{ij}^{disp} + u_{ij}^{HB} = \begin{cases} \infty & r < \sigma \\ -\varepsilon_1 - \varepsilon_{ij}^{HB}\sigma \le r < 1.2\sigma \\ -\varepsilon_2 & 1.2\sigma \le r < 1.5\sigma \\ -\varepsilon_3 & 1.5\sigma \le r < 1.8\sigma \\ -\varepsilon_4 & 1.8\sigma \le r < 2.0\sigma \\ 0 & r \ge 2.0\sigma \end{cases} \tag{5}$$

Equation 5 in conjunction with Table 1, including the bonded and nonbonded constraints construct the complete potential. Note that since hydrogen bonding forms between the two attractive sites within the cutoff distance r_c, the bonding to dimer formation has been restricted in the range of $\sigma - 2d_{site} < r_c \le \sqrt{\sigma^2 - \sqrt{3}\sigma d_{site} + d_{site}^2} - d_{site}$ after Jackson et al.,[15] where r_c is the cutoff distance for the hydrogen bonding attractive potential, d_{site} is the distance of the hydrogen bonded attractive site according to Figure 1. The range of hydrogen bonding interactions are $1 \le r^* < 1.2$ in this work, where $r^* = r/\sigma$ is dimensionless radial distance. In other words, the hydrogen bonded SW potential off-centered by a distance $d_{site} = 0.4\sigma$ and with a bonding range $r_c = 0.25\sigma$, in this article which satisfies the inequality criteria ($0.2\sigma < r_c = 0.25\sigma \le 0.28\sigma$). Thus, the O(carbonyl)—A bond and O(carbonyl)—C bond lengths are 0.1 nm (0.4×0.25) and likewise the O(hydroxyl)—A and O(hydroxyl)—C bond lengths are 0.1 nm (0.4×0.25). The distance between the bonded interaction sites could be constrained at 0.155 ± 0.015 nm, like the C—C distance in *n*-alkanes, and the angle between neighboring bonds could be constrained at $\sim 110^\circ$. The bonded constraints are characterized by covalently bound neighbors, L_{12}, and the next-nearest neighbors, L_{13}, that control the bond angles. The bond wells are specified by bond radii as $L_{ij} = R_{ijm} + R_{ijn}$, where L_{ij} is the center of the well, m and n specify the site type, and δ_{ij} specifies the breadth of the well based on $\delta_{ij} = R_{ijm}^{\delta} + R_{ijn}^{\delta}$. Therefore, the bond angle wells for O..(C)..O are $L_{13} = 0.255$ nm ($0.125 + 0.13$), for O(carbonyl)..(C)..C is $L_{13} = 0.256$ nm ($0.126 + 0.13$), and for O(hydroxyl)..(C)..C is 0.251 nm ($0.125 + 0.126$). The upper and lower values for these bonds are provided in a connectivity matrix, i.e., Table 2. σ_{intra}, influence

Table 1. New Site Types Specific to Carboxylic Acids and Default Definitions of Bonded Interaction Wells

Type	R_{12} (nm)	R_{12}^{δ}(nm)	R_{13} (nm)	R_{13}^{δ} (nm)	σ_{intra} (nm)	$(\varepsilon/k_B)_1$ (K)	$(\varepsilon/k_B)_4$ (K)	σ (nm)	K^{HB} (nm^3)	ε^{HB}/k_B (K)
Nonassociating sites										
CH_3—(C=)— acetic acid, e.g., 12 = CH_3…C, 13 = CH_3…=O or CH3…—OH—	0.075	0.008	0.125	0.013	0.275	43.789	43.789	0.363		
—CH_2—(C=)— n-aliphatic acids higher than acetic acid, e.g., 12 = CH_3…—CH_2 or —CH_2…C=, 13 = —CH_2…O= or —CH_2…—OH—	0.076	0.008	0.126	0.013	0.276	37.732	0.001	0.357		
=C in an ester or acid, e.g., 12 = C=… O or =C…—OH— or =C… —CH_2— or =C…CH_3 for acetic acid or =C… —CH_2 for *n*-aliphatic acids higher than acetic acid, 13 = =C…CH_3 for *n*-aliphatic acids higher than acetic acid	0.075	0.007	0.122	0.013	0.270	21.621	0.452	0.345		
Associating sites										
—OH—, e.g., 12 = —OH—…C=, 13 = —OH— … CH_2 for *n*-aliphatic acids higher than acetic acid, or —OH— O=, or —OH— … CH_3 for acetic acid	0.065	0.006	0.125	0.012	0.275	263.255	0.147	0.25	$2(10^{-4})$	251.6
=O, e.g., 12 = O=…C, 13 = =O… —OH—, or =O … CH_2 for n-aliphatic acids higher than acetic acid, or =O … CH_3 for acetic acid	0.062	0.006	0.130	0.013	0.286	97.827	0.706	0.25	$2(10^{-8})$	11323.6
Other nonassociating site types that are optimized as part of this work										
CH_3 ternary branch in 2,2-dimethyl propanoic acid, 12 = CH3…—C<, 13 = CH_3 … —C=O	0.075	0.008	0.125	0.012	0.275	40.496	37.383	0.363		
CH_2-(halogen) in chloroacetic acid, 12 = —CH_2…Cl or —CH_2…C=O, 13 = —CH_2…O= or CH_2…—OH—	0.076	0.008	0.126	0.013	0.276	17.396	17.371	0.357		
>CH in, e.g., i-butyric acid and i-valeric acid, e.g., in valeric acid, 12 = CH_3…CH or CH…—CH_2, 13 = CH…C=	0.076	0.008	0.128	0.013	0.283	6.948	2.554	0.39		
>C<F bonded to a acidic perfluoro, e.g., trifluoroacetic acid, 12 = >C<F…C=O, 13 = >C<F…O= or >C<F…—OH—	0.064	0.006	0.108	0.011	0.240	23.697	9.575	0.3425		
ACH aromatic CH, e.g., in benzoic acid, 12 = ACH…ACH or ACH…>AC=, 13 = ACH…ACH or ACH…>AC=	0.070	0.007	0.121	0.012	0.266	18.667	18.534	0.3425		
>AC = aromatic >C=, e.g., in benzoic acid, 12 = >AC=…ACH or >AC=…C=, 13 = >AC=…ACH or >AC=…O= or >AC=…—OH—	0.070	0.007	0.121	0.012	0.267	11.665	1.856	0.33		
=CH_2, e.g., in unsaturated carboxylic acids like acrylic acid and methacrylic acid, e.g., in methacrylic acid, =CH_2…=C<, 13 = =CH_2…C= or =CH_2…CH_3	0.067	0.007	0.133	0.013	0.293	55.753	8.967	0.35		
OH in a secondary acid-alcohol like lactic acid, 12 = OH…CH, 13 = OH…CH_3 or OH…C=	0.066	0.007	0.125	0.013	0.275	319.616	121.447	0.285		
Cl primary chloro in, e.g., Chloroacetic acid, 12 = Cl…CH_2, 13 = Cl…C=	0.099	0.010	0.143	0.014	0.314	140.230	13.603	0.333		

New site types specific to carboxylic acids. The bond wells are specified by bond radii as $L_{ij} = R_{ijm} + R_{ijn}$, where L_{ij} is the center of the well, m and n specify the site type, and δ_{ij} specifies the breadth of the well based on $\delta_{ij} = R_{ijm}^{\delta} + R_{ijn}^{\delta} \sim 0.05L_{ij}$.

Table 2. Upper and Lower Bounds of the Connectivity Matrix and Bond Angle Wells for Site Types Specific to Carboxylic Acids*

	Well 1		Well 2		Well 3	
Type	Low (nm)	High (nm)	Low (nm)	High (nm)	Low (nm)	High (nm)
CH_3—(C=) acetic acid	0.143	0.158	0.237	0.262	0.275	∞
—CH_2—(C=) n-aliphatic acids higher than acetic acid	0.144	0.159	0.238	0.263	0.276	∞
=C in an ester or acid	0.142	0.157	0.230	0.256	0.270	∞
Associating sites						
Type						
—OH—	0.122	0.135	0.237	0.262	0.275	∞
=O	0.121	0.133	0.246	0.272	0.286	∞
Other non-associating site types that are optimized as part of this work						
Type						
CH_3 ternary branch in 2,2-dimethyl propanoic acid	0.143	0.158	0.237	0.262	0.275	∞
CH_2-(halogen) in chloroacetic acid	0.144	0.159	0.238	0.263	0.276	∞
CH in, e.g., i-butyric acid and i-valeric acid	0.145	0.161	0.243	0.269	0.283	∞
>C<F bonded to a acidic perfluoro, e.g., trifluoroacetic acid	0.122	0.134	0.194	0.238		∞
ACH aromatic CH, e.g., in benzoic acid	0.132	0.146	0.229	0.253	0.266	∞
>AC= aromatic >C=, e.g., in benzoic acid	0.132	0.146	0.230	0.254	0.267	∞
$=CH_2$, e.g., in unsaturated carboxylic acids like acrylic acid and methacrylic acid	0.127	0.141	0.252	0.279	0.293	∞
OH in a secondary acid-alcohol like lactic acid	0.125	0.139	0.237	0.262	0.275	∞
Cl primary chloro in, e.g., chloroacetic acid	0.188	0.208	0.271	0.299	0.314	∞

*For example, for CH_3—(C=) R_{12}^{δ} = (well 1_{high} − well 1_{low})/2 = 0.008 nm, R_{12} = (well 1_{low} + R_{12}^{δ})/2 = 0.075 nm, R_{12}^{δ} = (well 2_{high} − well 2_{low})/2 = 0.012 nm, R_{13} = (well 1_{low} + R_{13}^{δ})/2 = 0.125 nm.

dihedral distributions, especially in the sense that cis-conformations are prevented. For instance, C=O and C—O bond lengths are 0.137 nm (0.075 + 0.062) and 0.14 nm (0.075 + 0.065) from Table 1. Note that the Note that the difference between C=O and C—O bond length is small to give the best value for the minimized potential energy of the entire molecule which is responsible for intramolecular interactions. A more robust algorithm for controlling the dihedral angle is beyond the scope of this work and will be reported later in our force-biased simulation approach. Intramolecular sites on the same molecule that are seven or fewer bonds apart are considered bonded and nonbonded interactions are the same for both intermolecular and intramolecular interactions that are seven bonds apart. The conventional rule in potentials that consider the dihedral angle explicitly (1–4 interaction) is to treat sites separated by four or more bonds as nonbonded interactions. However, for the SPEADMD the intramolecular force field is applied for the first seven bonds, in order to permit detailed specifications for highly branched and ring compounds.. Average MNDO (modified neglect of direct overlap, a semiempirical quantum mechanical method) optimization of the bond length and conformation for several typical compounds of the given functionality has been performed in order to determine values of L_{12} and L_{13} and to minimize the potential energy for the overall molecule. One can use also a general correlation between δ_{ij} and L_{ij} that is proposed in the previous work[22] as $\delta_{ij} = 0.05L_{ij}$. In this paper, 21 packing fraction ranging from 0.01 to 0.56 are used with 100 molecules per each density for simulation time of 2 ns. Note that periodic boundary condition and minimum image convention are implemented in the simulation box. Given a 2 ns of simulation time, the average number of contacts between CC sites is $125(10^6)$ at high packing fractions and is $35(10^6)$ at low packing fractions for acetic acid as an example.

SPEADMD equation of state and hydrogen bonding model

The simulations of each reference fluid lead to a complete equation of state (EOS) specific to that particular molecular structure. This EOS is essentially an interpolation between the state points of the available simulations, which can only be performed at a particular temperature, density, and composition. We outline below the specific set of equations for deriving the simulated properties and performing the interpolations.

Pure component EOS

SPEADMD applies the molecular simulation results for contribution of repulsive forces in the Helmholtz free energy (A0)and uses two version of the thermodynamic perturbation theory (TPT): (1) Barker-Henderson[60] TPT for the attractive dispersion interactions (A1, A2) and (2) Wertheim theory of association TPT for hydrogen bonding contribution (A^{assoc}).

$$\frac{A - A^{ig}}{RT} = A0 + \frac{A1}{T} + \frac{A2}{T^2} + \frac{A^{assoc}}{RT} \tag{6}$$

$$Z0(\eta, \vec{x}) = \sum_{i,j \text{ collided}} \left[\frac{\vec{F}_{ij} \Delta \vec{r}_{ij}}{3k_B T} \right] + \left\langle \frac{M \vec{v}_{ij} \Delta \vec{v}_{ij}}{3k_B T} \right\rangle \tag{7}$$

Note that $Z0$ can also be expressed in terms of packing fraction by an algebraic equation whose coefficients are determined from correlation of reference fluid compressibility factors.

$$Z0 = \frac{1 + z_1\eta + z_2\eta^2 + z_3\eta^3}{(1 - \eta)^3} \tag{8}$$

$$\left(\frac{A0(\eta,\vec{x})-A^{ig}}{kT}\right)_{T,V}=\int_0^{\eta}\frac{Z0-1}{\eta} \tag{9}$$

First and second order perturbation coefficients (A1 and A2) are to be computed from the general Barker and Henderson relationship[23]

$$A1=\frac{-1}{Nk_B}\sum_k\sum_l\sum_m\langle N_{klm}\rangle\varepsilon_{klm} \tag{10}$$

$$A2=\frac{-1}{2Nk_B^2}\sum_i\sum_j\sum_k\sum_l\sum_m\sum_n(\langle N_{ijm}N_{klm}\rangle - \langle N_{ijm}\rangle\langle N_{klm}\rangle)\,\varepsilon_{ijm}\varepsilon_{k\ln} \tag{11}$$

where an ensemble average is used for N_{ijm} which represents the number of pairs in the mth well of the ij interaction and N is the total number of molecules in the simulation. Likewise, as shown for Z0, A2 can also be calculated from a Pade approximation which is usually preferred to a polynomial approximation as shown by Gray et al.[40]

$$A2=\frac{a_{21}\eta+a_{22}\eta^2+a_{23}\eta^3+a_{24}\eta^4}{1+500\eta^4} \tag{12}$$

Currently, the SPEADMD EOS applies hydrogen bonding characterization in terms of sterospecific, short-range potentials which is quite consistent with Wertheim TPT theory.[13] Since our model uses multi-step potentials and hard spheres do not overlap, the potential can be made sufficiently short range that the formation of more than one bond at any given site is prohibited.

The result for binary association of pure fluids in terms of the Helmholtz energy can be expressed as

$$\frac{A^{assoc}}{RT}=\ln(X^A)+\frac{1-X^A}{2}+\ln(X^D)+\frac{1-X^D}{2}+\ln(X^C)+\frac{1-X^C}{2} \tag{13}$$

Note that X^A and X^D are determined from the bonding volume, X^{AD} and bonding energy, ε^{AD}.

To give more elaborations on the reliability of TPT for the extremely small association volume of the CC sites we should consider the analysis that has been performed by Busch and coworkers[42–44] and Chialvo et al.[61] As mentioned by Busch et al., carrying out explicit simulations for the full potential model becomes increasingly difficult as the strength of association increases. Traditional DMD and traditional Metropolis Monte Carlo methods do not provide reasonable statistics for carboxylic acids fluids which are strongly associated. However, the accuracy of TPT has been verified for larger bonding sites of varying size and bond energy (Joslin et al.,[62,63] Liu and Elliott[4]). Also, Chialvo et al. found that the properties of polar and associated systems such as carboxylic acids are determined by the repulsive interactions that can be used in perturbation expansions. Hence, we have a reasonable basis for extrapolating the theory to conditions where it is difficult to verify.

Finally, to study the association of carboxylic acids in both liquid and gas phases, we need to provide the structural information based on the radial distribution function (Section S.5 of the Supporting Information). We follow the procedure of Slovak and Nezbeda[64] based on TPT theory and define the full radial distribution function (rdf) by

$$g_{ij}=y_0\;e^{\frac{u_{ij}}{k_BT}}$$
$$y_0=g_{ij}^{ref}\;e^{\frac{u_{ij}^{ref}}{k_BT}} \tag{14}$$

where, u_{ij} ($=u_{ij}^{ref}+u_{ij}^{TPT1}$), u_{ij}^{ref}, and u_{ij}^{TPT1} are full potential, reference potential, and perturbed part of the potential, respectively. u_{ij}^{TPT1} is composed of dispersion as well as association parts, y_0 is the background correlation function, k_B is the Boltzman factor, T is the temperature, and g^{ref} is the reference fluid rdf. Briefly, this approach indicates a sharp spike in the rdf when the dimer is formed, as one would expect for a covalent dimer. This spike is exaggerated relative to what would be measured experimentally, partially because the bonding volume is set to an artificially low value in this model. If the rdf was a concern, it would be feasible to adapt this approach to correlate the rdf more accurately by applying a more disperse representation of the hydrogen bonding potential, such that the integral of the rdf yielded the same extent of dimerization as implied by the model. Enhanced dimerization relative to chain oligomerization is the key thermodynamic effect, however, so we have focused on that property in the current analysis.

Extension of the SPEADMD model to mixtures

Extensions of Wertheim's theory to mixtures as well as SPEADMD mixing rules are discussed in this subsection. Wertheim theory of association can be extended to mixtures according to the following relation

$$\frac{A^{assoc}}{RT}=\sum_i x_i\left[\begin{array}{l}Nd_i^A\left(\ln(X_i^A)+\frac{1-X_i^A}{2}\right)+Nd_i^D\left(\ln(X_i^D)+\frac{1-X_i^D}{2}\right)\\+Nd_i^C\left(\ln(X_i^C)+\frac{1-X_i^C}{2}\right)\end{array}\right] \tag{15}$$

where X_i^A is fraction of acceptors that are not bonded and Nd_i^j represents the degree (i.e., number of occurrences) of jth type in the ith species.

Gray and Elliott[65] provided a detailed analysis to obtain the best mixing rule for our equation of state. They found that the following equation gives the best results

$$AM=\frac{\sum_i\sum_j x_ix_jAM_{ij}(b_ib_j)^{1/2}}{\sum_i x_ib_i} \tag{16}$$

In Eq. 16 M refers to the order of the perturbation term (i.e., 0, 1, or 2), x_i the mole fraction of the ith component, and b_i is the molar volume of the ith molecule.

Table 3. Summary of % Deviations for Five Acids: Acetic, Propionic, i-Butyric, Pentanoic, and Octanoic

Method	ρ_L	VP	T_b	T_c
Clifford et al.	0.73	61.08	3.86	0.53
Kamath et al.	1.70	120.97	4.80	1.29
SPEADMD	3.92	24.25	1.52	6.61
SPEADCI	6.91	4.97	0.11	4.37

Notice that A0 effectively characterizes the athermal entropy of mixing and A1 and A2 characterize the energy of mixing.

In this work a self interaction parameter is defined to correct the vapor pressure error. The density-dependent binary interaction parameter for both like and unlike species is defined as

$$k_{ij} = k_{ij}^0 + k_{ij}^1 \eta \quad \text{for} \quad i = j \text{ and } i \neq j \tag{17}$$

For pure fluids ($i = j$), we have optimized both k_{ii}^0 and k_{ii}^1 to minimize the vapor pressure error. This results in a new model namely SPEADCI which has the capability of correlating pure and mixture properties with low deviations. The optimized values of k_{ii}^0 and k_{ii}^1 are given in Table 4 for all carboxylic acids used in this work.

As discussed by Vahid et al.[66] the SPEADMD model has a relatively large deviation in vapor pressure prediction due to transferability. Generally, transferability is a reasonable approximation but still an approximation, which results in deviation from experimental vapor pressure data. An alternative model (SPEADCI) can be formulated to customize the SPEADMD model for specific compounds. In this alternative, we alter the strength of the attractive perturbation by multiplying it by a customized interaction parameter by considering $A^{att} = A^{att}_{trans}(1-k_{ii})$. The detail of the intermolecular potentials is determined by estimation of $A1_{ij}$ since it has been recognized on a molecule–molecule (m-m) perspective in traditional thermodynamics. The energy of the mixture is defined using the m-m method and $A1_{ij}$ as:

$$Al_{ij} = (A1_i\ A1_j)^{1/2}(1 - k_{ij}^U) \tag{18}$$

It is also possible to describe the energy of mixing on a site–site (s-s) basis as has been considered by Sans and Elliott[67] for perfluorinated mixtures. The binary interaction parameter in the s-s perspective is more transferable, but still needs a detailed global optimization to characterize for more compounds. The mixture database used in this article is not comprehensive enough for a global optimization and hence this work only relies on the m-m analysis.

Results and Discussion

In this section, we provide a detailed discussion about characterization of carboxylic acids with the new optimized site types considered in this work. Also, the average absolute errors for carboxylic acids studied in this article are reported. Then, the peculiar vapor pressure and Z_V^{sat} trends for mono and dicarboxylic acids are discussed. Also, in section S.5 of the Supporting Information a discussion about the structural information and radial distribution of formic and acetic acids with current and other force fields as well as association in both liquid and vapor phases is given. As pointed out earlier, our model overestimates the association effects for small carboxylic acids. Hence, the performance of our model is compared to other force fields for carboxylic acids. Subsequently, VLE of aqueous carboxylic acid systems as well as acid + acid systems are evaluated with the current model. Finally, the LLE of water with two carboxylic acids (butyric and undecanoic) is considered with reference to separation processes.

Characterization of carboxylic acids

Linear aliphatic carboxylic acids greater than propionic acid have the general formula of $CH_3(CH_2)_nCOOH$. Therefore, all of the previous site types that had been optimized for all 35 families with our potential are considered transferable in this work. There are some special site types that are specific to carboxylic acid systems which are summarized in Table 1. The objective function below was minimized to obtain minimal deviations for vapor pressure, Z_V^{sat} and phase equilibria of all acids simultaneously while varying the parameters σ, ε_1, ε_4, ε^{AD}, and K^{AD} for the acid O= and OH site types.

$$OBF = \frac{\left|BP^{calc} - BP^{exp}\right|}{BP^{exp}} + \frac{\left|VP^{calc} - VP^{exp}\right|}{VP^{exp}} + \frac{\left|Z_V^{sat,calc} - Z_V^{sat,exp}\right|}{Z_V^{sat,exp}} \tag{19}$$

where BP is the mixture bubble pressure and VP is vapor pressure.

Dimerization energy and bonding volume were constrained by the following relations to the carbonyl oxygen's acceptor-donor values:

$$\varepsilon^{CC} = 3\varepsilon^{AD}_{O=} \tag{20}$$

$$K^{CC} = K^{AD}_{O=} \tag{21}$$

Note that the association effects are stronger in smaller acids because the aliphatic chains of higher acids dilute the association so that long chain carboxylic acids exhibit trends similar to high molecular weight n-alkanes. We also have considered the effect of enhanced accessibility for small acids due to steric hindrance and/or polarizability of the fluid but no substantial improvement in vapor pressure deviation was observed. This observation is consistent with our previous studies on amines[41] and alcohols.[48] The final value for the bonding volume of all carboxylic acids after several optimizations of the disperse interactions is $K^{AD} = 2(10^{-4})$ nm^3 for hydroxyl group and a very small value of $K^{CC} = 2(10^{-8})$ nm^3 for the carbonyl group in carboxylic acids. The strength of association is estimated by common rules[68–71] 21 kJ/mol for hydroxyl groups but we found that 2.1 kJ/mol, i.e., an order of magnitude less, provides a more accurate characterization of the balance between dimerization and chain formation for acids. Also, we should use a large value for the CC-type interactions i.e., $\varepsilon^{CC} = 94.1$ kJ/mol. This large

Table 4. Summary of Vapor Pressure Deviations for Carboxylic Acids Based on Conventional SPEADMD Model

Acid Training Set	Formula	SPEADMD %P AAD	SPEADMD %P Bias	SPEADMD %P Max	SPEADCI %P AAD	SPEADCI %P Bias	SPEADCI %P Max	Parameters in Eq. 17 k_{ii}^0	Parameters in Eq. 17 k_{ii}^1	T_{min}	η^{max}	No. of Pts
n-aliphatic acids												
Formic	CH_2O_2	18.8	−1.2	−44.4	1.6	−0.06	−4.2	−0.24	0.56	281.6	0.49	20
Acetic	$C_2H_4O_2$	11.6	3	−30	2.2	<0.01	6.5	−0.09	0.23	289.8	0.50	20
Propionic	$C_3H_6O_2$	8.6	8.5	12.3	0.7	−0.02	−1.9	−0.06	0.12	252.5	0.50	20
Butyric	$C_4H_8O_2$	18	−18	−24.5	0.8	<0.01	2.3	−0.01	0.07	267.9	0.48	20
Pentanoic	$C_5H_{10}O_2$	48.5	−48.5	−62	1.6	<0.01	4.1	−0.01	0.12	239.1	0.48	20
Heptanoic	$C_7H_{14}O_2$	49.1	−49.1	−79	4.9	−0.19	10.3	−0.18	0.58	265.8	0.48	20
Nonanoic	$C_9H_{18}O_2$	36.1	−4.8	83.5	6.2	−0.43	13.4	−0.98	2.29	285.5	0.48	22
Decanoic	$C_{10}H_{20}O_2$	39.4	14.8	99.7	4.1	−0.22	9.3	−0.53	1.52	304.5	0.47	20
Undecanoic	$C_{11}H_{22}O_2$	44.7	−43.5	−79.2	7.1	−0.67	15.8	−0.42	1.28	301.6	0.49	20
Tetradecanoic	$C_{14}H_{28}O_2$	45.5	4.2	105.6	1.1	−0.02	2.6	−0.53	1.59	327.4	0.47	20
Hexadecanoic	$C_{16}H_{32}O_2$	57.5	29	149.2	3	−0.14	−9.3	−0.5	1.42	335.7	0.46	20
Octadecanoic	$C_{18}H_{36}O_2$	27.8	−0.4	57	0.3	<0.01	−1.1	−0.51	1.42	342.7	0.46	20
Nonadecanoic	$C_{19}H_{38}O_2$	27.7	−27.7	−48.6	0.2	<0.01	0.3	−0.39	1.06	341.2	0.46	2
Dicarboxylic acids												
Adipic	$C_6H_{10}O_4$	63.2	1.1	160.6	5.9	−0.53	−15.2	−9.16	20.58	425.5	0.46	18
Pimelic	$C_7H_{12}O_4$	60.9	−60.9	−81.9	5.5	−0.48	−14.8	−20.62	47.12	379.1	0.47	20
Sebacic	$C_{10}H_{18}O_4$	40	−26.6	−74.9	5.2	−0.45	−14.8	−14.51	32.45	407.6	0.46	20
Unsaturated aliphatic acids												
Acrylic	$C_3H_4O_2$	8.5	8.5	12.1	0.5	<0.01	−1.4	−0.07	0.14	395.4	0.48	20
Methacrylic	$C_4H_6O_2$	20.3	−18.7	−39.6	2.9	−0.07	6.7	−0.23	0.7	288.1	0.48	20
Oleic	$C_{18}H_{34}O_2$	69.1	−69.1	−95.5	2.6	−0.08	−8.7	−0.37	1.18	286.5	0.49	20
Aromatic acids												
Benzoic	$C_7H_6O_2$	40.8	−40.8	−66.9	2.8	−0.08	6.4	−0.35	0.93	286.1	0.52	20
Cinnamic	$C_9H_8O_2$	23.7	23.7	52.4	1	−0.01	2.3	−0.62	1.53	406.1	0.48	20
Chloro acids												
Chloroacetic	$C_2H_3ClO_2$	6.8	0.5	15.1	1.3	<0.01	3.3	−0.13	0.31	333.1	0.48	20
Hydroxy acids												
Lactic	$C_3H_6O_3$	0.4	0.4	0.4	0.1	<0.01	0.1	0.15	−0.3	289.9	0.53	1
Fluoro acids												
Trifluoroacetic	$C_2HF_3O_2$	11.6	1.2	−26.3	1.3	−0.04	−3.4	−0.15	0.36	257.9	0.50	20
Branched saturated aliphatic acids												
2-ethyl butyric	$C_6H_{12}O_2$	69	−69	−70.2	0.7	−0.01	−1	−2.74	6.98	258.1	0.44	3
2-methylhexanoic	$C_7H_{14}O_2$	67.7	−67.7	−67.7	4.4	−0.22	7.5	−0.08	0.46	230	0.49	6
2,2-dimethyl propanoic	$C_5H_{10}O_2$	6.2	−1	16.9	1.8	−0.01	4.3	0.09	−0.21	309.8	0.47	20
i-valeric	$C_5H_{10}O_2$	3.9	3.7	11.5	1.2	<0.01	3.2	−0.07	0.14	243.8	0.50	20
Cyclic aliphatic acids												
Cyclopentylacetic	$C_7H_{12}O_2$	37.2	−37.2	−44	2.4	−0.08	−5.2	−0.18	0.43	286.6	0.49	8
Average training set		33.6	−17.1		2.5	−0.13						500
Validation set												
n-aliphatic acids												
Hexanoic	$C_6H_{12}O_2$	44.9	−44.9	−72.8	6.4	−0.26	15.4	−0.12	0.39	269.2	0.48	20
Octanoic	$C_8H_{16}O_2$	51.2	−51.2	−81.5	6.2	−0.39	13.6	−0.26	0.8	289.6	0.48	20
Dodecanoic	$C_{12}H_{24}O_2$	38.5	−19.8	−72.8	2.1	−0.07	5.7	−0.52	1.61	317	0.49	20
Tridecanoic	$C_{13}H_{26}O_2$	43.6	−10.8	84.9	2.8	−0.1	7.3	−0.55	1.75	293	0.47	20
Pentadecanoic	$C_{15}H_{30}O_2$	53.7	14.1	137.2	1.5	−0.04	−3.8	−0.55	1.68	293.1	0.47	20
Heptadecanoic	$C_{17}H_{34}O_2$	55.3	24.4	141.7	3	−0.15	−9.7	−0.49	1.4	334.2	0.46	19
Dicarboxylic acids												
Suberic	$C_8H_{14}O_4$	56.2	−56.2	−80.5	5.5	−0.56	15.3	−18.75	42.58	416.1	0.47	20
Azelaic	$C_9H_{16}O_4$	54.3	−18.5	107	5.5	−0.58	15.7	−8.53	18.91	379.6	0.48	15
Branched saturated aliphatic acids												
i-butyric	$C_4H_8O_2$	41.8	−41.8	−48.1	1.2	<0.01	3	0.05	−0.07	227.1	0.50	20
2-ethylhexanoic	$C_8H_{16}O_2$	62.6	−62.1	−97.3	0.2	<0.01	0.2	−0.13	0.55	213.1	0.43	20
Average validation set		51.5	−23.4		3.4	−0.21						194
Average total		42.5	−20.3		3	−0.17						694

Experimental data are taken from DIPPR compilation.

value combines with the small bonding volume to generate significant dimerization at low temperature, but rapidly weakening dimerization with increasing temperature, in accordance with an exothermic reaction.

Kamath et al.[36] and Clifford et al.[38] used a point-charge force field which overpredicts the vapor pressure with more than 50% average absolute deviation (% AAD) for relatively small carboxylic acids including acetic, propionic, i-butyric,

pentanoic, and octanoic acids. Also, Kamath et al.[36] have reported a large positive vapor pressure bias for various potentials such as OPLS-AA and CHARMM. They mentioned that these large errors contributed to the parameterization of the various functional groups in the potential as well as molecular aspect ratio $L^* = L/\sigma$, where L is the site–site separating distance and σ is the collisional diameter. We believe, however, that all of these point-charge force fields suffer by neglecting the distinct nature of dimerization as a reaction.

Table 3 summarizes the results for vapor pressure, critical properties, normal boiling points, and liquid densities, comparing the SPEADMD model to the models of Kamath et al.[36] and Clifford et al.[38] for five acids: acetic, propionic, i-butyric, pentanoic, and octanoic. These five acids were selected for comparison because they were included in all three databases. Briefly, the SPEADMD model is less accurate for liquid density and much more accurate for vapor pressure. The average absolute error for liquid density for the SPEADMD model is 4.4% for the entire carboxylic acid family. This article is primarily devoted to phase equilibria (VLE and LLE). Therefore, vapor pressure error receives greater emphasis than liquid density. Liquid density may be more important for transport properties.[59,72]

Critical properties are estimated according to the law of rectilinear diameter[73] in combination with a scaling exponent β. The best scaling was found to be $\beta = 0.29$ for acids with chain length between 1 to 10 as well as all dicarboxylic acids, and $\beta = 0.325$ for higher acids, consistent with works of Clifford et al.[38] and Chen et al.[74] Details of these properties are given in Section S.5.1 and Tables S3–S17 of the Supporting Information.

Table 4 summarizes vapor pressure and density errors for a large database of carboxylic acids based on the DIPPR compilation, restricting the range of conditions to temperatures at which experimental vapor pressures were available. Note that the overall percent absolute average error (AAD%) for vapor pressure is 34.7% for training compounds and 49.8% for validation compounds. Also, the small deviations in liquid density support the site diameters that have been chosen in this work. The total AAD% of the liquid density is 4.3% which is small enough for our present carboxylic acid model. Table 4 also shows the results of the customized interaction model, i.e., SPEADCI, for the same database. Note that the SPEADCI model corrects for vapor pressure and the largest vapor pressure error is 5.9 AAD% while the average vapor pressure error is 2.8 AAD%.

The results from Tables 3 show that the dicarboxylic acid compounds have the largest vapor pressure errors. Also, a strange jump in vapor pressure bias appears when the chain length is increased from decanoic acid to undecanoic acid. This is related to the discrepancy between the experimental data of these two acids. Basically, the experimental data (that are from two different sources) jump from decanoic acid to undecanoic acid and hence, the bias has a significant decrease in this transition. The model, on the other hand, has a smooth transition behavior for the entire family of carboxylic acids.

Pure fluid analysis

A systematic analysis has been performed to correlate vapor pressure and vapor density of carboxylic acids with transferable potentials. The vapor pressure trends for pure carboxylic acids are presented in Figure 2 as well as Table 4 based on the transferable SPEADMD model. According to Table 4 and Figure 2, the vapor pressure curve becomes steeper as the molecular weight of carboxylic acid becomes larger. On the other hand, the vapor pressure bias is more negative for larger compounds. This general behavior has been previously observed by Unlu et al.[48] for straight-chain alcohols. Overall, the SPEADMD model underestimates the heat of vaporization in accordance with the Clausius-Clapeyron equation given below

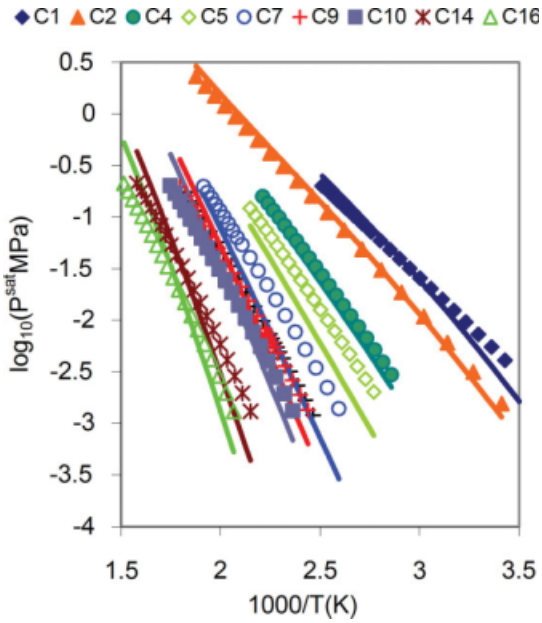

Figure 2. Vapor pressure prediction of SPEADMD model for aliphatic carboxylic acid (training compounds) systems ranging from C1 to C16.

[Color figure can be viewed in the online issue, which is available at www.interscience.wiley.com.]

$$\log\left(\frac{P^{\text{sat}}}{P_{\text{ref}}}\right) \cong -\frac{\Delta H_{\text{vap}}}{R}\left(\frac{1}{T} - \frac{1}{T_{\text{ref}}}\right) \tag{22}$$

Also, the vapor pressure results are more accurate at higher temperatures, which is consistent with findings of Kamath et al.[36] and Clifford et al.[38] The bias for dicarboxylic acids is highly negative due to super strong association in the vapor phase and as discussed later, these particular multifunctional carboxylic acids behave like high molecular weight monocarboxylic acids. The large negative bias also means that we have overestimated the strength of association which was necessary in order to obtain accurate VLE results for carboxylic acid/water system.

The variations of Z_V^{sat} for several carboxylic acids are plotted in Figure 3. As depicted in Figure 3 (Experimental data are from Vargaftik et al.[75] for acetic acid and from Miyamoto et al.[76] for propionic, butyric, and pentanoic acid) a large negative deviation ($Z < 1$) from ideal gas behavior

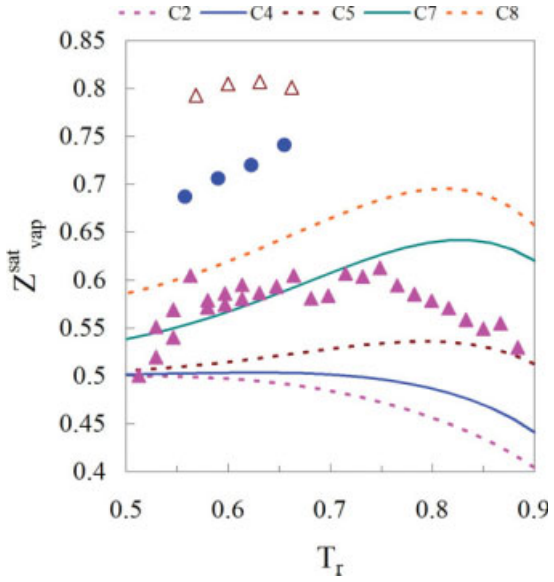

Figure 3. Variation of saturated vapor compressibility factor for C2–C8 aliphatic acids.

Experimental data from Vargaftik et al.[75] and from Miyamoto et al.[76] for acetic acid ▲, butyric ●, and pentanoic acids △. [Color figure can be viewed in the online issue, which is available at www.interscience.wiley.com.]

occurs due to strong dimerization in small monocarboxylic acids even at low pressures. Acids have this unusual tendency to dimerize even at low pressures well below 1 bar. Other common associated fluids such as alcohols, aldehydes, esters, etc. have noticeable amounts of dimerization at normal pressures (close to 1 bar), but do not exhibit such small Z_V^{sat} at lower pressures. Complex formation by association or solvation is negligible at low pressures because the fraction of dimerization goes to zero as pressure approaches zero for nonacids.[77] In smaller acids, the increasing dimerization due to temperature decrease of the exothermic reaction overwhelms the weakening dimerization from the saturated vapor density decrease. It is also clear that the association dilutes as the chain length increases. Hence, carboxylic acids with higher molecular weights have higher compressibility factor owing to weaker association. For higher acids, the saturation temperature naturally is higher due to disperse interactions, in addition to the dilution effect. Notice that there is there is a significant difference between the experimental data and predicted values of Z_{vap}^{sat} for acetic, propionic, butyric, and pentanoic acid, however. This is attributed to the overestimating of the association in the vapor phase in order to give optimum results for vapor pressure, Z_V^{sat}, and VLE.

For more clarification, we have tested a larger bonding volume and a smaller association energy for the CC interaction consistent with the general guidelines,[71] previous simulations,[78–80] and experiments[81–83] ($K^{AD} = 2(10^{-5})$ nm^3, $\varepsilon^{CC} = 62 \pm 2$ kJ/mol) and demonstrated the results in section S2 of the Supporting Information (Tables S1, S2, Figure S8) in order to explain the best possible tradeoff of the parameterization of the current model. Although the results for the vapor compressibility factor are improved especially for acetic acid, the vapor pressure (36.9% AAD for vapor pressure of C_1–C_5), and VLE results (11.4% AAD for bubble pressure of aqueous carboxylic acid mixtures) are not reliable and the VLE diagrams are not qualitatively correct. Furthermore, at this stage, it seems that the four site water model used in this work ($\varepsilon^{HB} = 13.3$ kJ/mol, $K^{AD} = 1.8(10^{-3})$ nm^3) needs to be revised in the future in a manner that a more reasonable hydrogen bonding energy for carbonyl oxygen can be used. For instance, Müller et al.[84] and McCallum et al.[85] have used a higher hydrogen bonding energy along with a lower hydrogen bonding volume ($\varepsilon^{HB} = 31.6$ kJ/mol, $K^{AD} = 1.2(10^{-4})$ nm^3) in their four site water model. Their model has been evaluated for adsorption of water on activated carbon containing acetic acid not for bulk binary mixture of carboxylic acids + water, however. Their model needs to be tested and compared with more advanced models[86–89] supported with X-ray and neutron scattering measurements of the structure of liquid water.[90,91] We refer the reader to Appendix A for the discussion about the interesting and peculiar behavior of dicarboxylic acids in their vapor compressibility factors.

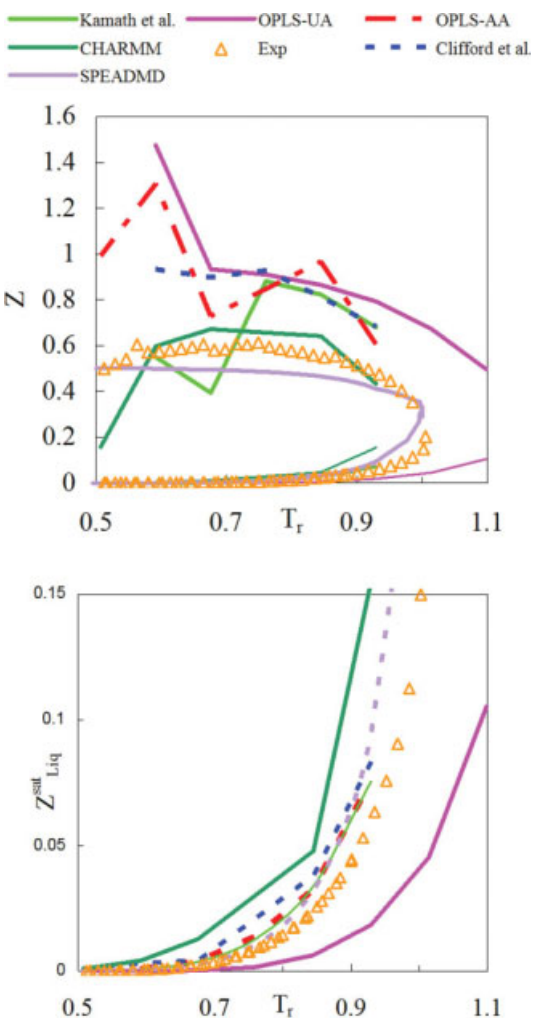

Figure 4. Vapor–liquid coexistence curves for acetic acid.

Several potential models are compared against experimental data that are taken from Vargaftik and coworkers.[75] [Color figure can be viewed in the online issue, which is available at www.interscience.wiley.com.]

Table 5. Detailed VLE Results for Carboxylic Acid Mixture Systems

System				% AAD P			
ID1	ID2	Component 1	Component 2	NDP	SPEADMD	SPEADCI	NRTL
			Carbox/Water				
1921	1251	Water	Formic acid	139	6.18	1.99	0.71
1921	1252	Water	Acetic acid	381	2.77	1.29	0.72
1921	1253	Water	Propionic acid	147	6.20	4.35	1.90
1921	1256	Water	Butyric acid	62	5.19	4.30	2.76
1921	1277	Water	Acrylic acid	44	4.64	4.44	1.56
1921	1278	Water	Methacrylic acid	35	4.95	1.79	1.13
		Average Carbox/Water		808	4.36	2.39	1.15
			Carbox/Carbox				
1251	1252	Formic acid	Acetic acid	198	6.02	2.85	1.60
1251	1253	Formic acid	Propionic acid	58	5.48	1.71	1.14
1251	1256	Formic acid	Butyric acid	5	9.71	1.54	1.32
1251	1258	Formic acid	Pentanoic acid	45	14.33	3.68	2.08
1252	1253	Acetic acid	Propionic acid	104	2.37	0.97	0.88
1252	1256	Acetic acid	Butyric acid	6	8.53	3.85	2.84
1252	1277	Acetic acid	Acrylic acid	48	2.61	0.84	0.52
1253	1256	Propionic acid	Butyric acid	57	7.15	1.02	0.85
1253	1258	Propionic acid	Pentanoic acid	48	13.48	1.87	1.42
1253	1870	Propionic acid	Trifluoroacetic acid	19	4.58	1.79	0.86
1256	1260	Butyric acid	i-butyric acid	10	8.69	1.76	1.59
1256	1261	Butyric acid	i-valeric acid	9	17.00	3.97	2.85
1258	1260	Pentanoic acid	i-butyric acid	48	11.08	1.35	1.15
1262	1265	Hexanoic acid	Octnanoic acid	83	24.92	2.40	1.32
1265	1254	Octanoic acid	Decanoic acid	18	20.06	1.51	1.32
1269	1271	Dodecanoic acid	Tetradecanoic acid	26	32.92	2.03	1.77
1271	1272	Tetradecanoic acid	Hexadecanoic acid	24	27.08	1.89	1.45
		Average Carbox/Carbox		814	10.51	2.01	1.31
			Carbox/*N*-Alkane				
1252	1	Acetic acid	Methane	46	3.47	3.19	2.55
1269	1	Dodecanoic acid	Methane	15	2.37	1.24	1.83
1252	11	Acetic acid	*n*-Hexane	9	7.12	3.77	2.85
1253	11	Propionic acid	*n*-Hexane	9	5.66	3.33	1.68
1252	17	Acetic acid	*n*-Heptane	65	4.07	2.34	1.49
1253	17	Propionic acid	*n*-Heptane	42	1.45	1.29	1.17
1256	17	Butyric acid	*n*-Heptane	30	7.44	3.64	2.44
1258	17	Pentanoic acid	*n*-Heptane	65	7.52	3.69	2.51
1252	27	Acetic acid	*n*-Octane	39	3.12	2.36	1.85
1253	27	Propionic acid	*n*-Octane	54	5.32	3.04	1.52
		Average Carbox/*N*-Alkane		374	4.75	2.79	1.99
		Average Total		1996	6.54	2.39	1.48

NDP, number of data points.[70–139]

A comparison of various force fields against experimental data is illustrated in Figure 4 for acetic acid's Z_V^{sat}. The SPEADMD model is the best one in predicting both liquid and vapor phase properties. For other acids, the general behavior is the same and the results are given in the Supporting Information (Figures S2–S7). The main reason for the excellent behavior of the SPEADMD model in both phases is attributed to having Wertheim's theory in its background, which is specifically designed for chemical reaction that occurs during hydrogen bonding. Other models are basically point-charge approaches in which the strong hydrogen bonding has not been treated explicitly. The association in these point-charge approaches has been implemented implicitly through assigning special charges to each site type. Some of these models exhibit strong dimerization but most do not, as illustrated in Figure 4. However, if one allows a point-charge model to have several parameters that use various sets of partial charges for acid–acid and acid–water intermolecular interactions, then one could also improve the agreement with experiment implicitly. Overall, the SPEADMD EOS has qualitative rather than quantitative capability to predict Z_V^{sat}, (due to overestimating the strength of association). But the coverage of mixture VLE and multiple acids with a single transferable model is distinctive. Possible sources of further improvement might include combined point charge + reactive modeling, an enhanced quantum mechanical approach, or altering the bonding sites as in the 1A scheme of Muro-Suñé and coworkers.[6–9,32,33]

Finally, the heat of vaporization of acetic acid should exhibit a maximum when plotted against temperature (Figure S16 of the Supporting Information), but this is not encompassed by the present model. This maximum in H^{vap} is related to the maximum in Z_V^{sat}, as described by the Clapeyron equation. It is possible to represent this maximum by choosing a smaller value for the ε^{CC} of acetic acid, but such a low value of ε^{CC} cannot be transferred to other acids to achieve a generally optimal characterization of vapor pressure. Once again, the current model represents a broadly applicable basis for all carboxylic acids, but customized descriptions for specific acids can be envisioned with adaptations of parameters like ε^{CC}.

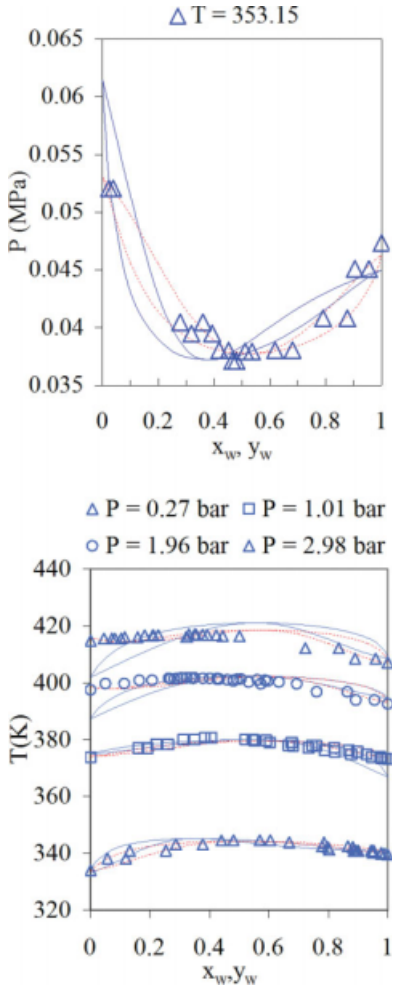

Figure 5. VLE predictions for the water + formic acid binary system (k_{ij} = −0.06) using the SPEADMD (solid blue lines) and SPEADCI (dashed red lines).

Data are from Gmehling et al.[94] [Color figure can be viewed in the online issue, which is available at www.interscience.wiley.com.]

Mixture results

We have considered 33 binary systems of carboxylic acids + water, carboxylic acid + carboxylic acid, and acids + n-alkane. In our data collection, an electronic database, i.e., EVLM[92] has been referenced, which contains the citation of the experimental data from the year of 1888 until 2004. The Korean database[93] and DECHEMA[94] series as well as literature data[70,76,95–139] were referenced.

The results of VLE calculations are presented in Table 5 where a two parameter NRTL model is used to compare with SPEADMD and SPEADCI. The total absolute deviations in bubble pressure are 4.4% for SPEADMD, 2.4% for SPEADCI, and 1.1% for NRTL based on carboxylic acids/water systems while for carboxylic acids/carboxylic acids systems these errors are 10.5%, 2%, and 1.3% for SPEADMD, SPEADCI, and NRTL, respectively. Also, to perform a more systematic test of transferability we have analyzed binary mixtures with a nonassociated compound such as an n-alkane. The total absolute deviations in bubble pressure are 4.7% for SPEADMD, 2.8% for SPEADCI, and 2% for NRTL in this situation. The total AAD% of bubble point pressure is 6.5% for SPEADMD, 2.4% for SPEADCI, and 1.5% for NRTL. The results of the SPEADCI approach are close to the NRTL model and the deviations are similar in magnitude to the deviations in correlating the pure component vapor pressure. Table 5 indicates that VLE accuracy diminishes as we go to higher molecular weight acids. This observation is also consistent with the vapor pressure correlation. VLE graphs for selected carboxylic acid mixtures are provided in Figures 5 and 6. As discussed earlier, the SPEADMD model approximately correlates the overall vapor pressures of carboxylic acids because of transferability. The SPEADCI approach could be used to refine precision in cases when data were available. Figure 5 shows the VLE phase diagram for the water + formic acid system over a broad range of temperatures and pressures. Formic acid is the simplest and smallest carboxylic acid, with strong association in both liquid and vapor phases. Formic acid has an extremely small critical compressibility factor of $Z_c = 0.149$ which verifies this strong association. This acid most likely forms a cyclic dimer rather than polymeric chain aggregates in the vapor phase. Notice that a strong solvation of the carboxylic hydroxyl in acids with water is observed for all water/carboxylic acids systems with the solvation energy of $\varepsilon_{ij}^{HB} = 67.1$ kJ/mol and solvation binary interaction of $k_{ij}^{AD} = -0.8$ for carboxylic hydroxyl-water interactions and $k_{ij}^{AD} = 0$ for carbonyl oxygen-water interactions in Eq. 4. This system has been studied by Grenzheuser et al.[5] with the PHC equation of state and UNIQUAC activity coefficient model. They obtained excellent result (0.7% PAAD) within the same range of temperatures and compositions but their model suffers from lack of transferable potentials, physicochemical consideration of hydrogen bonding, and neglecting the association term in the liquid phase.

Figures 6 and S9 of the Supporting Information present the solvation of acetic acid in water from considerably low pressure, 0.27 bar, to an elevated high pressure of 21.7 bar. This system exhibits positive deviations from ideality. This system has also been considered by several authors including Grenzheuser and Gmehling,[5] Kouskoumvekaki et al.,[140] Wolbach and Sandler,[29] and Perakis et al.[34] These authors used a one site association model (1A) for carboxylic acids and their association model for water is not consistent and varies with the system of interest. The best binary interaction parameter is $k_{ij} = -0.052$, with 2% PAAD for SPEADCI. Figure 6a is instructive regarding the presence of a pinch point at low acetic acid concentration, which constrains the recovery of acetic acid from water. The strong solvation between water + acetic acid (carboxylic hydroxyl with water) can be described by Eq. 4 with a large negative value for $k_{ij}^{AD} = -0.95$ for carboxylic hydroxyl-water interactions, $k_{ij}^{AD} = 0$ for carbonyl oxygen-water interactions, and $\varepsilon_{ij}^{HB} = 68.2$ kJ/mol at $T = 462.1$ K. Note that a higher solvation energy and a more negative value for the solvation binary interaction parameter has been chosen to mimic the pinch behavior of this mixture in a robust fashion. Figure S22 of section S.6 of the Supporting Information shows the general qualitative trend of the VLE of water + acetic acid using the old values for solvation interactions (used for Figures 5

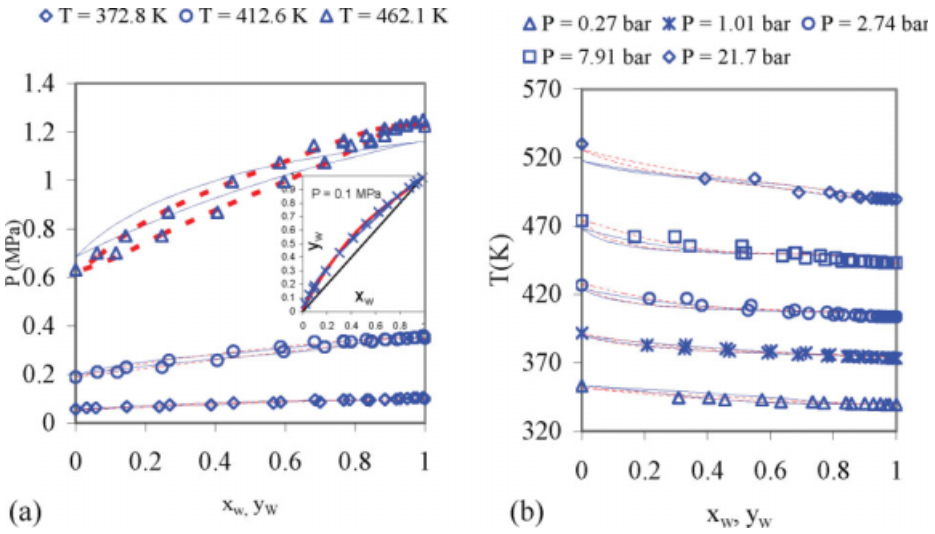

Figure 6. VLE prediction for the water + acetic acid binary system ($k_{ij} = -0.052$) using the SPEADMD (solid blue lines) and SPEADCI (dashed red lines).

Experimental data are taken from Freeman et al.[97] (a), Othmer et al.[105] and Gmehling et al.[94] (b). [Color figure can be viewed in the online issue, which is available at www.interscience.wiley.com.]

and 6b) at 462.1 K. Muro-Suñé et al.[33] underestimate the solvation strength by considering a zero value for k_{ij}^{AD}. Also, it seems that the multiple association site type scheme considered in this work, gives quantitative results when compared with the VLE graph which is presented by Muro-Suñé et al. It is worthwhile mentioning that our model gives satisfactory results with considering only one binary interaction parameter whereas Muro-Suñé et al. model gives qualitative results based on a one parameter van der Waals mixing rule. Furthermore, when they use a local composition excess Gibbs energy Huron-Vidal mixing rule with the cost of more adjustable parameters at broad ranges of temperature, the improved results are still qualitative when the relative volatility approaches unity. The water + acrylic acid system is interesting since it has relatively large deviations of bubble pressure error for both SPEADMD and SPEADCI equations of state. This large error is attributed to the unusually strong association of the acrylic acid. Figure S10 of the Supporting Information shows positive deviations from ideality.

In mixtures containing two carboxylic acids, the association is still complicated because of the solvation that occurs between the two acids. The solvation energy in this case is 94 kJ/mol for CC acid/acid interactions with $k_{ij}^{CC} = 0$ in for CC interactions in Eq. 4. Acid/acid mixtures generally have ideal solution behavior except for systems containing formic acid. Figure S11 of the Supporting Information shows the VLE graph for formic acid + acetic acid system at low pressures. SPEADMD fails to predict the vapor pressure of formic acid as obvious in Figures S11 and S12 of the Supporting Information. This behavior is expected due to formic acid high tendency to associate in both phases especially vapor phase. Figure S11 of the Supporting Information is another example that verifies the strong association of formic acid in the vapor phase.

Figure S13 of the Supporting Information illustrates the phase diagram of the mixture of two highly associated acids, i.e., acetic acid and acrylic acid. There is ideal solvation between these two acids and both SPEADMD and SPEADCI give satisfactory results.

As we go to higher molecular weight acids such as butyric, pentanoic…decanoic, and so on, the behavior of mixtures moves toward ideal solution behavior, similar to n-alkanes. This is expected because the association effect becomes weaker as the chain length grows. Note that for these high molecular weight acids the vapor pressure prediction of the SPEADMD model has a large error and the SPEADCI model is preferable. Examples of such binary carboxylic acid + carboxylic acid mixtures are given in Figures S14 and S15 of the Supporting Information. An interesting system is propionic + pentanoic acid which has generally positive deviations from Raoult's law but small negative deviations in the pentanoic acid rich region. This is a special characteristic of carboxylic acid + carboxylic acid binary mixtures and is related to considerable formation of heterodimer according to Tamir et al.[112–114] and Clifford et al.[122,141]

Finally, in order to test the reliability of the model for predicting liquid–liquid equilibria (LLE), two typical systems of i-butyric acid + water and undecanoic acid + water were considered and presented in Figures B1 and B2 of Appendix. Both SPEADMD and SPEADCI give satisfactory results with a negative value of binary interaction parameter $k_{ij} \sim -0.1$. Also, the correlation of models for extremely immiscible system such as undecanoic acid + water gives a reasonable value of $k_{ij} \sim -0.05$.

Conclusions

With this work, we characterize the anomalous behavior of carboxylic acids resulting from their strong association in both liquid and vapor phases by using simultaneous phase equilibria and chemical reaction according to an adaptation of Wertheim's theory for carboxylic acids. Simultaneously

correlating the vapor compressibility factor, its trend with molecular weight, and VLE behavior for acid and alcohol mixtures necessitates compromises in terms of theoretical and experimental accuracy. For example, the vapor pressure errors are three times larger than other SPEADMD potentials when applying a completely transferable model of acid bonding, and larger still for dicarboxylic acids. In order to correct for the vapor pressure and obtain acceptable phase equilibria results for mixtures, customized interaction model (SPEADCI) can be employed for pure fluids. Also, solvation is observed to be substantial for acid + water and acid + acid systems. Despite these compromises, the SPEADCI model is comparable in accuracy to the best available methods for acids, even while those methods may be specialized to ignore one or more of the peculiar behaviors of acid systems. Having a universal model helps to clarify the true nature of the molecular interactions in acids and sets the stage for further refinements that enhance precision without sacrificing the accuracy of the global perspective. Finally, the future study should focus on extending the SPEAD model to systems with long-range interactions such as polar fluids which have some important properties like dielectric constant. This goal is achievable by implementing a field-biased approach into our simulation method and treating Coulombic interactions through Ewald summation. This goal is the subject of current research. With such methods we would be able to study self-assembly aggregation phenomena at interfaces as has been done by Chen et al.[142]

Acknowledgments

This research was supported in part by Chemstations Inc., Houston, TX.

Notation

%AAD = (100/#Pts) × Σ |calculated − measured|, where #Pts refers to the number of measured points
A0 = reference part of the thermodynamic perturbation theory (TPT)
A1 = first-order term of the TPT, attractive-dispersion Helmholtz energy
A2 = second-order term of the TPT, attractive-dispersion Helmholtz energy
A^{assoc} = association Helmholtz energy computed from Wertheim theory
BP = bubble point pressure
d_{site} = distance of the hydrogen bonded attractive site, nm
F_{ij} = site-site force, N
g_{ij} = pair correlation function, radial distribution function
ΔH^{vap} = heat of vaporization, kJ/mol
i, j = site types
k_B = Boltzman factor ≈ 1.381×10^{-23} J/K
k_{ij} = molecule-molecule binary interaction parameter
k_{ij}^{AD} = site-site solvation interaction parameter
k_{ij}^{ss} = site-site binary interaction parameter
K^{AD} = AD hydrogen bonding volume, nm^3
K^{CC} = CC hydrogen bonding volume, nm^3
L = site-site separating distance, nm
$L_{ij} = R_{ijm} + R_{ijn}$, nm L_{ij} = the center of the bond well, nm L_{12}-covalent bounded neighbors, nm
L_{13} = next nearest neighbors, nm
M = mass, kg
MNDO = modified neglect of direct overlap
N_A = number of proton acceptors per bonding site
N_D = number of proton donors per bonding site
N_C = number of carboxylic sites per bonding site
N_d = number of hydrogen bonding segments per molecule
N_{ijm} = number of pairs in the mth well of the ij interaction and N is the total number of molecules in the simulation
P = pressure, MPa
r_c = cutoff distance for the hydrogen bonding attractive potential, nm
R_{ijm} = the bond radii of site type m, nm
R_{ijm}^{δ} = the radius of the ijth well on the mth site type, nm
Δr_{ij} = site-site distance, nm
rdf = radial distribution function
SPEADMD = step potential equilibria and dynamics, molecular dynamic version
SPEADCI = step potential equilibria and dynamics with a customized interaction parameter
T = temperature, K
TPT = thermodynamic perturbation theory
u_{ij} = potential energy
VP = vapor pressure
v = molecular velocity, nm/s
X^A = mole fraction of molecules NOT bonded at site A
Y_{CC} = carboxylic attractive energy parameter = $\exp(\beta\varepsilon^{CC}) - 1$
y_0 = background correlation function of the reference fluid
Z_0 = reference fluid compressibility factor
Z = compressibility factor

Greek letters

α_{CC} = carboxylic affinity factor = $\eta Y_{CC}(1 - \eta/2)/(1 - \eta)^3$
β = rectilinear critical scaling power
$\delta_{ij} = R_{ijm}^{\delta} + R_{ijn}^{\delta}$ = the breadth of the well
ε_{ijm} = site type potential energy of the mth well
ε_{ij}^{AD} = bonding energy of an acceptor on the ith site with a donor on the jth site, kJ/mol
ε^{HB} = hydrogen bonding energy, kJ/mol
ε^{CC} = hydrogen bonding energy of dimerizing sites, kJ/mol
η = packing fraction
σ = site type diameter, nm

Superscripts

assoc = association
AD = acceptor-donor site
CC = carboxylic-carboxylic site
disp = dispersion
HB = hydrogen bonding
sat = saturated

Subscripts

liq = liquid
ref = reference
V = vapro
vap = vaporization in the enthalpy formula

Literature Cited

1. Williams RB. Biofuels from Municipal Wastes-Background Discussion Paper. Available at: http://biomass.ucdavis.edu/materials/reports%20and%20publications/2007/2007_Annual_Forum_Background_Paper.pdf (accessed on March 6, 2008).
2. Elliott JR, Lira CT. *Introductory Chemical Engineering Thermodynamics*, *1st ed*. Englewood Cliffs, NH: Prentice-Hall, 1999.
3. Sandler SI. *Chemical, Biochemical, and Engineering Thermodynamics*, *4th ed*. New York: Wiley, 2006.

4. Liu J-X, Elliott JR. Screening effects on hydrogen bonding in chain molecular fluids: thermodynamics and kinetics. *Ind Eng Chem Res.* 1996;35:2369–2377.
5. Grenzheuser P, Gmehling J. An equation of state for the description of phase-equilibria and caloric quantities on the basis of the chemical theory. *Fluid Phase Equilib.* 1986;25:1–29.
6. Derawi SO, Zeuthen J, Michelsen ML, Stenby EH, Kontogeorgis GM. Application of the CPA equation of state to organic acids. *Fluid Phase Equilib.* 2004;225:107–113.
7. Folas GK, Derawi SO, Michelsen ML, Stenby EH, Kontogeorgis GM. Recent application of the cubic-plus-association (CPA) equation of state to industrially important systems. *Fluid Phase Equilib.* 2005;228–229:121–126.
8. Kontogeorgis GM, Michelsen M, Folas GK, Derawi S, von Solms N, Stenby EH. Ten years with the CPA (Cubic-Plus-Association) equation of state, Part 1: Pure compounds and self-associating systems. *Ind Eng Chem Res.* 2006;45:4855–4868.
9. Kontogeorgis GM, Michelsen ML, Folas GK, Derawi S, von Solms N, Stenby EH. Ten years with the CPA (Cubic-Plus-Association) equation of state, Part 2: Cross-associating and multicomponent systems. *Ind Eng Chem Res.* 2006;45:4869–4878.
10. von Solms N, Michelsen ML, Passos CP, Derawi SO, Kontogeorgis GM. Investigating models for associating fluids using spectroscopy. *Ind Eng Chem Res.* 2006;45:5368–5374.
11. Braga D, Maini L, Fagnano C, Taddei P, Chierotti MR, Gobetto R. Polymorphism in crystalline cinchomeronic acid. *Chem Eur J.* 2007;13:1222–1230.
12. Gavezzotti A, Filippini G, Kroon J, vanEijck BP, Klewinghaus P. The crystal polymorphism of tetrolic acid (CH3C CCOOH): a molecular dynamics study of precursors in solution, and a crystal structure generation. *Chem Eur J.* 1997;3:893–899.
13. Wertheim MS. Fluids with highly directional attractive forces. II. Thermodynamic perturbation theory and integral equation. *J Stat Phys.* 1984;35:35–47.
14. Chapman WG, Jackson G, Gubbins KE. Phase-equilibria of associating fluids chain molecules with multiple bonding sites. *Mol Phys.* 1988;65:1057–1079.
15. Jackson D, Chapman WG, Gubbins KE. Phase equilibria of associating fluids: spherical molecules with multiple bonding sites. *Mol Phys.* 1988;65:1–31.
16. Emami FS, Vahid A, Elliott JR, Feyzi F. Group contribution prediction of vapor pressure with statistical associating fluid theory, perturbed-chain statistical associating fluid theory, and Elliott-Suresh-Donohue equations of state. *Ind Eng Chem Res.* 2008; 47:8401–8411.
17. Huang S, Radosz M. Equation of state for small, large, polydisperse, and associating molecules. *Ind Eng Chem Res.* 1990; 29:2284.
18. Michelsen ML, Mollerup JM. *Thermodynamic Models: Fundamentals and Computational Aspects*. Copenhagen, Denmark: Tie-Line Publications, 2004.
19. Tihic A, Kontogeorgis GM, von Sohns N, Michelsen ML, Constantinou L. A predictive group-contribution simplified PC-SAFT equation of state: application to polymer systems. *Ind Eng Chem Res.* 2008;47:5092–5101.
20. Gross J, Sadowski G. Perturbed-Chain SAFT: an equation of state based on a perturbation theory for chain molecules. *Ind Eng Chem Res.* 2001;40:1244–1260.
21. Elliott JR, Natarajan RN. Extension of the ESD equation to polymer solutions. *Ind Chem Eng Res.* 2002;41:1043.
22. Elliott JR, Vahid A, Sans AD. Transferable potentials for mixed alcohol-amine interactions. *Fluid Phase Equilib.* 2007;256:4–13.
23. Barker JA, Henderson D. Perturbation theory and equation of state for fluids: the square-well potential. *J Chem Phys.* 1967; 47:2856.
24. Sear RP, Jackson G. Thermodynamic perturbation theory for association into chains and rings. *Phys Rev E.* 1994;50:386–394.
25. Sear RP, Jackson G. The ring integral in a thermodynamic perturbation theory for association. *Mol Phys.* 1996;87:517–521.
26. Tsonopoulos C, Prausnitz JM. Fugacity coefficients in vapor-phase mixtures of water and carboxylic acids. *Chem Eng J.* 1970;273–278.
27. Wolbach JP, Sandler SI. Thermodynamics of hydrogen bonding from molecular orbital theory. II. Organics. *AIChE J.* 1997;43: 1597–1604.
28. Wolbach JP, Sandler SI. Thermodynamics of hydrogen bonding from molecular orbital theory. I. Water. *AIChE J.* 1997;43:1589–1596.
29. Wolbach JP, Sandler SI. Using molecular orbital calculations to describe the phase behavior of cross-associating mixtures. *Ind Eng Chem Res.* 1998;37:2917–2928.
30. Colominas C, Teixido J, Cemeli J, Luque FJ, Orozco M. Dimerization of carboxylic acids: reliability of theoretical calculations and the effect of solvent. *J Phys Chem B.* 1998;102:2269–2276.
31. Huang S, Radosz M. Equation of state for small, large, polydisperse, and associating molecules: extension to fluid mixtures. *Ind Eng Chem Res.* 1991;30:1994.
32. von Solms N, Kouskoumvekaki IA, Michelsen ML, Kontogeorgis GM. Capabilities, limitations and challenges of a simplified PC-SAFT equation of state. *Fluid Phase Equilib.* 2006;241:344–353.
33. Muro-Suñé N, Kontogeorgis GM, von Solms N, Michelsen ML. Phase equilibrium modelling for mixtures with acetic acid using an association equation of state. *Ind Eng Chem Res.* 2008;47:5660–5668.
34. Perakis CA, Voutsas EC, Magoulas KG, Tassios DP. Thermodynamic modeling of the water + acetic acid + CO2 system: the importance of the number of association sites of water and of the nonassociation contribution for the CPA and SAFT-type models. *Ind Eng Chem Res.* 2007;46:932–938.
35. Gross J, Sadowski G. Application of the perturbed-chain SAFT equation of state to associating systems. *Ind Eng Chem Res.* 2002;41:5510–5515.
36. Kamath G, Cao F, Potoff JJ. An improved force field for the prediction of the vapor-liquid equilibria for carboxylic acids. *J Phys Chem B.* 2004;108:14130–14136.
37. Kamath G, Potoff JJ. Partial charge assignments in the force field characterization of acetic acid. In: *Midwest Thermodynamics and Statistical Mechanics Symposium*, West Lafayette, IN, 2005.
38. Clifford SL, Bolton K, Ramjugernath D. Monte Carlo simulation of carboxylic acid phase equilibria. *J Phys Chem B.* 2006; 110:21938–21943.
39. Schnabel T, Cortada M, Vrabec J, Lago S, Hasse H. Molecular model for formic acid adjusted to vapor-liquid equilibria. *Chem Phys Lett.* 2007;435:268–272.
40. Gray NH, Gerek ZN, Elliott JR. Molecular modeling of isomer effects in naphthenic and aromatic hydrocarbons. *Fluid Phase Equilib.* 2005;228–229:147–153.
41. Baskaya FS, Gray NH, Gerek ZN, Elliott JR. Transferable step potentials for amines, amides, acetates, and ketones. *Fluid Phase Equilib.* 2005;236:42–52.
42. Busch NA, Wertheim MS, Chiew YC, Yarmush ML. A Monte-Carlo method for simulating associating fluids. *J Chem Phys.* 1994;101:3147–3156.
43. Busch NA, Chiew YC, Yarmush ML, Wertheim MS. Development and validation of a simple antigen-antibody model. *AIChE J.* 1995;41:974–984.
44. Busch NA, Wertheim MS, Yarmush ML. Monte Carlo simulation of n-member associating fluids: application to antigen-antibody systems. *J Chem Phys.* 1996;104:3962–3975.
45. Elliott JR, Gerek ZN, Gray NH. Combining molecular dynamics and chemical process simulation: the SPEAD model. *Asia-Pacific J Chem Eng.* 2007;2:257–271.
46. Wertheim MS. Thermodynamic perturbation theory of polymerization. *J Chem Phys.* 1987;87:7323.
47. Cui J, Elliott JR Jr. Phase diagrams for multi-step potential models of n-alkanes by discontinuous molecular dynamics/ thermodynamic perturbation theory. *J Chem Phys.* 2002;116: 8625.
48. Unlu O, Gray N, Gerek ZN, Elliott JR. Transferable step potentials for the straight chain alkanes, alkenes, alkynes, ethers, and alcohols. *Ind Eng Chem Res.* 2004;43:1788–1793.
49. Ucyigitler S, Camurdan MC, Turkay M, Elliott JR. Inferring transferable intermolecular potential models. *Mol Simul.* 2008; 34:147–154.
50. Hansen J-P, McDonald IR. *Theory of Simple Liquids*, *3rd ed.* Amsterdam: Academic Press, 2006.
51. Chapman WG, Gubbins KE, Jackson G, Radosz M. New reference equation of state for associating liquids. *Ind Chem Eng Res.* 1990;29:1709.
52. Vlcek L, Nezbeda I. From realistic to simple models of associating fluids. II. Primitive models of ammonia, ethanol and models of water revisited. *Mol Phys.* 2004;102:485–497.

53. Picaud S. Dynamics of TIP5P and TIP4P/ice potentials. *J Chem Phys*. 2006;125:174712.
54. Lisal M, Kolafa J, Nezbeda I. An examination of the five-site potential (TIP5P) for water. *J Chem Phys*. 2002;117:8892–8897.
55. Alder BJ, Wainright TE. Studies in molecular dynamics. I. General methods. *J Chem Phys*. 1959;31:459.
56. Rapaport DC. The event scheduling problem in molecular dynamic simulation. *J Comput Phys*. 1980;34:184.
57. Liu J-X, Bowman TL II, Elliott JR Jr. Discontinuous molecular dynamics simulation of hydrogen-bonding systems. *Ind Eng Chem Res*. 1994;33:957.
58. Smith SW, Hall CK, Freeman BD. Molecular dynamics for polymeric fluids using discontinuous potentials. *J Comp Phys*. 1997;134:16–30.
59. Rapaport DC. *The Art of Molecular Dynamics Simulation*, *2nd ed*. New York: Cambridge University Press, 2004.
60. McQuarrie DA. *Statistical Mechanics*, *2nd ed*. New York: University Science Books, 2000.
61. Chialvo AA, Kettler M, Nezbeda I. Effect of the range of interactions on the properties of fluids. II. Structure and phase behavior of acetonitrile, hydrogen fluoride, and formic acid. *J Phys Chem B*. 2005;109:9736–9750.
62. Joslin CG, Gray CG, Chapman WG, Gubbins KE. Theory and simulation of associating liquid-mixtures. 2. *Mol Phys*. 1987;62:843–860.
63. Joslin CG, Gray CG, Gubbins KE. Renormalized perturbation-theory for dipolar and quadrupolar polarizable liquids. *Mol Phys*. 1985;54:1117–1128.
64. Slovak J, Nezbeda I. Extended five-site primitive models of water: theory and computer simulations. *Mol Phys*. 1997;91: 1125–1136.
65. Gray NH, Elliott JR. Quadratic mixing in perturbation theory. In: *AIChE Fall National Meeting*, Austin, TX, 2004, 160e.
66. Vahid A, Sans AD, Elliott JR. Correlation of mixture vapor-liquid equilibria with the SPEADMD model. *Ind Eng Chem Res*. 2008;47:7955–7964.
67. Sans AD, Elliott JR. Transferable potentials for perfluorinated molecules. *Fluid Phase Equilib*. 2008;263:182–189.
68. Durr J, Maurer G. Linear solvation energy relationship parameters of some pure liquid organic compounds from solvatochromic investigations. *Fluid Phase Equilib*. 2001;186:123–149.
69. Kamlet MJ, Abboud JM, Abraham MH, Taft RW. Linear solvation energy relationships. 23. A comprehensive collection of the solvatochromic parameters, pi*, alpha, and beta, and some methods for simplifying the generalized solvatochromic equation. *J Org Chem*. 1983;48:2877–2887.
70. Marcus Y. The properties of organic liquids that are relevant to their use as solvating solvents. *Chem Soc Rev*. 1993;22:409–416.
71. Pimentel GC, McClellan AL. *The Hydrogen Bond*, *1st ed*. New York: Reinhold, 1960.
72. Frenkel D, Smit B. *Understanding Molecular Simulation: From Algorithms to Applications*, *2nd ed*. San Diego: Academic Press, 2002.
73. Kofke DA. Direct evaluation of phase coexistence by molecular simulation via integration along saturation line. *J Chem Phys*. 1993;98:4149.
74. Chen B, Potoff JJ, Siepmann JI. Monte Carlo calculations for alcohols and their mixtures with alkanes. Transferable potentials for phase equilibria. 5. United-atom description of primary, secondary, and tertiary alcohols. *J Phys Chem B*. 2001;105:3093–3104.
75. Vargaftik NB, Vinogradov YK, Yargin VS. *Handbook of Physical Properties of Liquids and Gases: Pure Substances and Mixtures*, *3rd ed*. New York: Begell House, 1996.
76. Miyamoto S, Nakamura S, Iwai Y, Arai Y. Measurement of vapor-phase compressibility factors of monocarboxylic acids using a flow type apparatus and their association constants. *J Chem Eng Data*. 1999;44:48.
77. Prausnitz JM, Lichtenthaler RN, Azevedo EG. *Molecular Thermodynamics of Fluid-Phase Equilibria*, *3rd ed*. New Jersey: Prentice-Hall, 1999.
78. Gao JL. Comparison of the hybrid Am1/Tip3p and the Opls functions through Monte-Carlo simulations of acetic-acid in water. *J Phys Chem*. 1992;96:6432–6439.
79. Briggs JM, Nguyen TB, Jorgensen WL. Monte-Carlo simulations of liquid acetic-acid and methyl acetate with the Opls potential functions. *J Phys Chem*. 1991;95:3315–3322.
80. Picaud S, Hoang PNM, Peybernes N, Le Calve S, Mirabel P. Adsorption of acetic acid on ice: experiments and molecular dynamics simulations. *J Chem Phys*. 2005;122:194707.
81. Frurip DJ, Curtiss LA, Blander M. Vapor-phase association in acetic and trifluoroacetic acids—thermal-conductivity measurements and molecular-orbital calculations. *J Am Chem Soc*. 1980;102:2610–2616.
82. Jing C, Bruno JZ. Ideal gas thermodynamic properties of methanoic and ethanoic acids. *J Phys Chem Ref Data*. 1978;7: 363–377.
83. Claque ADH, Bernstein HJ. The heat of dimerization of some carboxylic acids in the vapour phase determined by a spectroscopic method. *Spectrochim Acta*. 1969;25A:593–596.
84. Müller EA, Rull LF, Vega LF, Gubbins KE. Adsorption of water on activated carbons: a molecular simulation study. *J Phys Chem*. 1996;100:1189–1196.
85. McCallum CL, Bandosz TJ, McGrother SC, Müller EA, Gubbins KE. A molecular model for adsorption of water on activated carbon: comparison of simulation and experiment. *Langmuir*. 1999;15:533–544.
86. Mahoney MW, Jorgensen WL. A five-site model for liquid water and the reproduction of the density anomaly by rigid, nonpolarizable potential functions. *J Chem Phys*. 2000;112: 8910–8922.
87. Guillot B. A reappraisal of what we have learnt during three decades of computer simulations on water. *J Mol Liq*. 2002;101:219–260.
88. Sanz E, Vega C, Abascal JLF, MacDowell LG. Phase diagram of water from computer simulation. *Phys Rev Lett*. 2004;92:255701.
89. Lombardero M, Martin G, Jorge S, Lado F, Lomba E. An integral equation study of a simple point charge model of water. *J Chem Phys*. 1999;110:1148–1153.
90. Sorenson JM, Hura G, Glaeser RM, Head-Gordon T. What can x-ray scattering tell us about the radial distribution functions of water? *J Chem Phys*. 2000;113:9149–9161.
91. Soper AK, Rossky PJ. Liquid water and aqueous solutions—preface. *Chem Phys*. 2000;258:107–108.
92. Wichterle I, Linek J, Wagner Z, Kehiaian HV. *Vapor-Liquid Equilibrium in Mixtures and Solutions Bibliographic Database: EVLM'2003* (Electronic ed., Version 5.0, 1888–2003 edition). Paris: Eldata, 2004.
93. Lee CS. Korean Database, Thermodynamics and Properties Lab. Available at: http://infosys.korea.ac.kr/kdb/index.html (accessed on January 1, 2008).
94. Gmehling J, Onken U, Arlt W. *DECHEMA Chemistry Data Series, Vol. 1: Vapor Liquid Equilibrium Data Collection*. Germany: Frankfurt, 1981–1996.
95. Conti JJ, Othmer DF, Gilmont R. Composition of vapors from boiling binary solutions. Systems containing formic acid, acetic acid, water, and chloroform. *Chem Eng Data*. 1960;5: 301–307.
96. Ito T, Yoshida F. Vapor-liquid equilibria of water-lower fatty acid systems: water-formic acid, water acetic acid and water-propionic acid. *J Chem Eng Data*. 1963;8:315–320.
97. Freeman JR, Wilson GM. High temperature PVT properties of acetic acid/water mixtures. *AIChE Symp Ser*. 1985;81:1–13.
98. Cruz JL, Renon H. Nonideality in weak binary electrolytic solutions. Vapor-liquid equilibrium data and discussion of the system water-acetic acid. *Ind Eng Chem Fundam*. 1979;18:168–174.
99. Sebastiani E, Lacquaniti L. Acetic acid-water system thermodynamical correlation of vapor-liquid equilibrium data. *Chem Eng Sci*. 1967;22:1155–1162.
100. Haddad PO, Edmister WC. Phase equilibriums in acetic acid-diethylketone-water system. *J Chem Eng Data*. 1972;17:275–278.
101. Narayana AS, Naik SC, Rath P. Salt effect in isobaric vapor-liquid equilibria of acetic acid-water system. *J Chem Eng Data*. 1985;30:483–485.
102. Vercher E, Vazquez MI, Martinez-Andreu A. Isobaric vapor-liquid equilibria for water + acetic acid + lithium acetate. *Ind Eng Chem*. 2001;46:1584–1588.
103. Abraham MA, Klein MT. Pyrolysis of benzylphenylamine neat and with tetralin, methanolm and water solvents. *Ind Eng Chem Res*. 1985;24:300–306.
104. Ramalho RS, James WJ, Carnaham JF. Effect of alkaline-earth chloride on vapor-liquid equilibrium of acetic acid-water system. *J Chem Eng Data*. 1964;9:215–217.
105. Othmer DF, Silvis SJ, Spiel A. Composition of vapors from boiling binary solutions; pressure equilibrium still for studying water-acetic acid system. *Ind Eng Chem*. 1952;44:1864.

106. Aristovich VY, Levin AI. *Vses Nauchn Issled Inst Neftekhim Protsessov*. 1962;5:84.
107. Hunsmann W, Simmrock KH. Separation of water, formic acid and acetic acid by azeotrope distillation. *Chem Ing Tech*. 1966;38:1053–1059.
108. Hunsmann W. Verdampfungsgleichgewicht von Ameisensäure/Essigsäure-und von Tetrachlorkohlenstoff/Perchloräthylen-Gemischen. *Chem Ing Tech*. 1967;39:1142–1145.
109. Alpert N, Elving PJ. Vapor-liquid equilibria in binary systems. Ethylene dichloride-toluene and formic acid-acetic acid. *Ind Eng Chem*. 1949;41:2864–2867.
110. Kato M, Yamaguchl M, Yoshikawa H. Vapor-liquid equilibria at 100 kPa for propionic acid + carbon tetrachloride or 2-butanone. *J Chem Eng Data*. 1990;35:85–87.
111. Kato M, Yoshikawa H, Yamaguchi M. Vapor-liquid measurements of three binary systems made of formic acid, acetic acid and propionic acid by the dew-bubble point temperature method. *Fluid Phase Equilib*. 1990;54:47–56.
112. Tamir A, Dragoescu C, Apelblat AW. Heats of vaporization and vapor-liquid equilibria in associated solutions containing formic acid, acetic acid, propionic acid and carbon tetrachloride. *Fluid Phase Equilib*. 1983;10:9–42.
113. Tamir A, Wisniak J. Vapor equilibrium in associating systems (water-formic acid-propionic acid). *Ind Eng Chem Fundam*. 1976;15:274–280.
114. Tamir A, Wisniak J. Vapor-liquid equilibria in association solutions. *Chem Eng Sci*. 1975;30:335–342.
115. Kushner TM, Tatsievskaya GI, Iruzun VA, Volkova LV, Serafimov LA. Liquid-vapor phase equilibrium in the water-formic acid-acetic acid system under 50 and 200 mm. Hg pressure. *Zh Fiz Khim*. 1966;40:3010–3017.
116. Chubarov GA, Danov SM, Brovkina GV. Liquid-vapor equilibrium in butyl alcohol-acrylic acid, propyl alcohol-acrylic acid, water-acrylic acid, and acetic acid-acrylic acid systems. *Zh Prikl Khim (Sankt-Petersburg, Russian Federation)*. 1976;49:1413–1415.
117. Linek J, Wichterle L. Liquid-vapor equilibrium. LX. System acetic acid-acrylic acid at 200 Torr. *Coll Czech Chem Commun*. 1973;38:1853–1857.
118. Trybula S, Bandrowski J. Liquid-vapor equilibrium in binary systems of carboxylic acids. *Inz Chem*. 1975;5:679–695.
119. Giles NF, Wilson GM. Vapor-liquid equilibria on four binary systems: 2-Phenylpropionaldehyde + phenol, propylene glycol monomethyl ether + nitroethane, dimethyl ether + propylene, and N-butyric acid + propionic acid. *J Chem Eng Data*. 2006;51: 1966–1972.
120. Sewnarain R, Ramjugernath D, Raal JD. Isobaric vapor-liquid equilibria for the systems propionic acid + butyric acid, isobutyric acid + butyric acid, butyric acid + isovaleric acid, and butyric acid + hexanoic acid at 14 kPa. *J Chem Eng Data*. 2002;47:603–607.
121. Jonescu I, Savescu V, Cioroianu D, Simoiu L, Mehmedinteanu L. Liquid-vapor equilibrium data for binary mixtures of propionic acid, butyric acid and butyl acetate and models critically selected for design purposes. *L Rev Roum de Chim*. 1998;38: 457–462.
122. Clifford SL, Ramjugernath D, Raal JD. Vapour-liquid equilibrium of carboxylic acid systems: propionic acid + valeric acid and isobutyric acid + valeric acid. *Fluid Phase Equilib*. 2005; 237:89–99.
123. Malijevska I. Liquid-vapor equilibrium. Part LXXIX. Liquid-vapor equilibrium in the strongly associating system propionic acid-trifluoroacetic acid. *Coll Czech Chem Comm*. 1978;43:2225–2232.
124. Akiya N, Savage PE. Roles of water for chemical reactions in high-temperature water. *Chem Rev*. 2002;102:2725–2750.
125. Müller E. *Exp. Vermessung von Dampffluessigkeit-Phasengleichgen*. Berlin, Heidelberg: Springer-Verlag, 1961; Stage F1:1.
126. Müller E. *Exp. Vermessung von Dampffluessigkeit-Phasengleichgen*. Berlin, Heidelberg: Springer-Verlag, 1961; Stage H.:1.
127. Müller E. *Exp. Vermessung von Dampffluessigkeit-Phasengleichgen*. Berlin, Heidelberg: Springer-Verlag, 1961; Stage I-I:1.
128. Jonasson A, Persson O, Rasmussen P, Soave GS. Vapor-liquid equilibria of systems containing acetic acid and gaseous components. Measurements and calculations by a cubic equation of state. *Fluid Phase Equilib*. 1998;152:67–94.
129. Shy DS, Yau JS, Tsai FN. Phase-behavior of methane with carboxylic-acids. *J Chem Eng Data*. 1993;38:112–115.
130. Miyamoto S, Nakamura S, Iwai Y, Arai Y. Measurement of isothermal vapor-liquid equilibria for hydrocarbon plus monocarboxylic acid binary systems by a flow-type apparatus. *J Chem Eng Data*. 2000;45:857–861.
131. Lark BS, Banipal TS, Singh S. Excess Gibbs energy for binary-mixtures containing carboxylic-acids. 3. Excess Gibbs energy for isobutyric acid and trimethylacetic acid + cyclohexane and + N-heptane. *J Chem Eng Data*. 1987;32:402–406.
132. Markuzin NP, Pavlova LM. Liquid-vapor equilibriums in an acetic acid-heptane-toluene system. I. Experimental data based on equilibrium in binary systems and a calculation of the dimerization constant for acetic acid in the vapor. *Zh Prikl Khim (Sankt-Petersburg, Russian Federation)*. 1971;44:311–315.
133. Nerner G. J. *Prakt Chew*. 1965;29:26.
134. Plesnar Z, Fu YH, Sandler SI, Orbey H. Vapor-liquid equilibrium of the acetic acid plus octane binary system at 323.15 K and 343.15 K. *J Chem Eng Data*. 1996;41:799–801.
135. Zieborak K, Srzostowski I. *Rocz Chem*. 1953;32:1145.
136. Johnson AI, Ward DM, Furter WF. Vapor-liquid equilibrium data for system: octane-propionic acid, with salt effect. *Can J Tech*. 1957;34:514–518.
137. Rothmund V. The mutual solubility of liquids and the critical point of solution. *Z Phys Chem*. 1898;26:433–492.
138. Friedländer J. About strange features in the environment of the critical point partial of mixable liquids. *Z Phys Chem*. 1901;38:385–440.
139. Soares ME, Medina AG, Bailes PJ. Liquid liquid equilibria of the system water isobutyric acid cumene. *Fluid Phase Equilib*. 1983;15:91–105.
140. Kouskoumvekaki IA, Krooshof GJP, Michelsen ML, Kontogeorgis GM. Application of the simplified PC-SAFT equation of state to the vapor-liquid equilibria of binary and ternary mixtures of Polyamide 6 with several solvents. *Ind Eng Chem Res*. 2004;43:826–834.
141. Naumova AA, Tyvina TN. Liquid-liquid phase equilibrium in the water-undecanoic acid-pyridine system. *Zh Prikl Khim (Sankt-Petersburg, Russian Federation)*. 1982;55:2330–2332.
142. Chen J, Brooks CL, Scheraga HA. Revisiting the carboxylic acid dimers in aqueous solution: Interplay of hydrogen bonding, hydrophobic interactions, and entropy. *J Phys Chem B*. 2008;112:242–249.

Appendix A: Dicarboxylic acids' peculiar behavior

Figure A1 shows that dicarboxylic acids have larger compressibility factors in comparison with monocarboxylic acids at low reduced temperatures which may seem surprising at first glance. Similar to higher acids, the compressibility

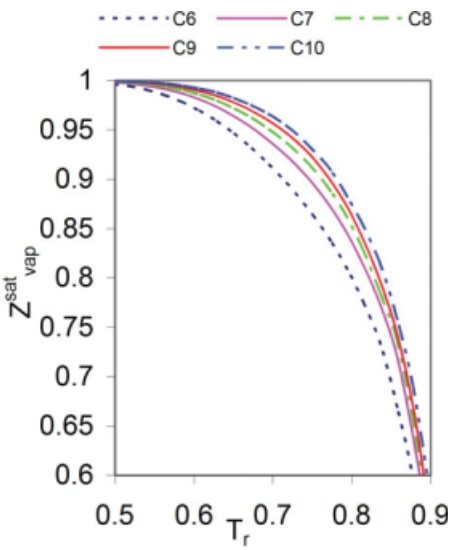

Figure A1. Variation of saturated vapor compressibility factor for dicarboxylic acids.

[Color figure can be viewed in the online issue, which is available at www.interscience.wiley.com.]

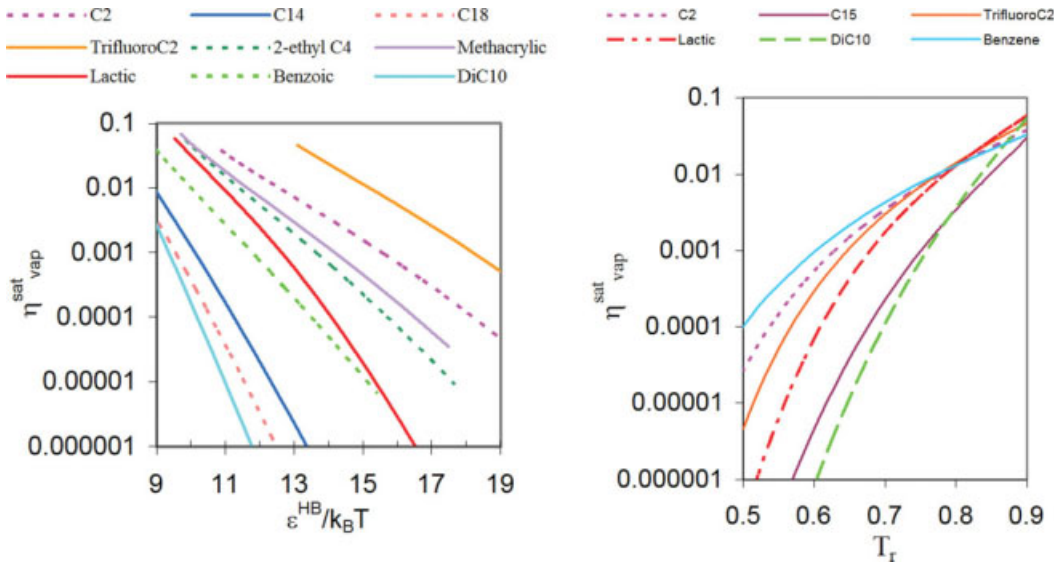

Figure A2. Behavior of the saturated-vapor packing fraction at different temperatures for various carboxylic acids families.

[Color figure can be viewed in the online issue, which is available at www.interscience.wiley.com.]

factors of dicarboxylic acids approach unity because their saturation temperatures are so high. These systems have higher saturation temperatures and lower saturated-vapor packing fractions as depicted in Figure A2. The affinity factor [$\alpha_{CC} = \eta Y_{CC}(1 - \eta/2)/(1 - \eta)^3$] reflects the combined influences of temperature and density. Figure A3 shows the strength of association vs. reduced temperature which emphasizes that dicarboxylic acids behave similar to high molecular weight monocarboxylic acids.

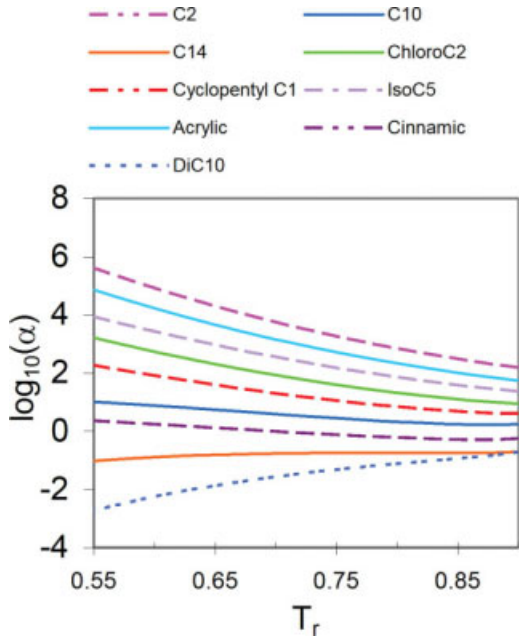

Figure A3. Plot of the affinity factor vs. reduced temperature for various carboxylic acids families.

[Color figure can be viewed in the online issue, which is available at www.interscience.wiley.com.]

Note that Figures 3, A1–A3 show that our model overestimates the energy of hydrogen bonding but as mentioned earlier this is inevitable since this large hydrogen bonding energy is required for robust VLE predictions. These figures show that as the affinity factor ($\boldsymbol{\alpha}$) and saturated-vapor packing fraction ($\boldsymbol{\eta}^{sat}_{vap}$) decreases, the strength of association (Y^{HB}) increases which means that the dicarboxylic acid compounds have a strong association in both liquid and vapor phases. Also the right hand side of the Figure A2 shows that the general behavior of η^{sat}_{vap} is similar for acetic acid and benzene. This is related to the vapor pressure and compressibility factor of benzene and acetic acid according to the following equation

$$\eta^{sat}_{vap} = \frac{Pb}{ZRT} \tag{A1}$$

where b is the volumetric size parameter. According to general databases the critical temperature of benzene and acetic acid are close to each other and the compressibility factor of benzene is close to unity since it does not dimerize. Moreover, it is a low molecular weight compound and its vapor pressure is higher than acetic acid but the compressibility factor for acetic acid is lower than benzene. All of these effects will result in a similar behavior of the saturated-vapor packing fraction vs. reduced temperature.

Appendix B: Liquid-liquid equilibria graphs

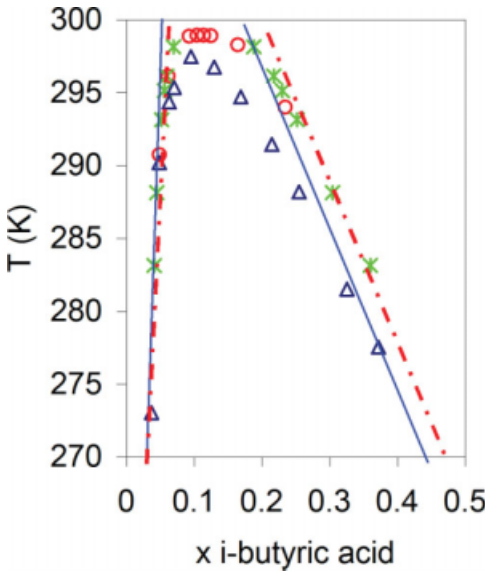

Figure B1. LLE graph for the i-butyric acid + water binary system (k_{ij} = −0.1) using the SPEADMD (solid blue lines) and SPEADCI (dashed red lines).

Experimental data are taken from Rothmund et al.[137] △, Friedlaender et al.[138] ○, and Soares et al.[139] (*). [Color figure can be viewed in the online issue, which is available at www.interscience.wiley.com.]

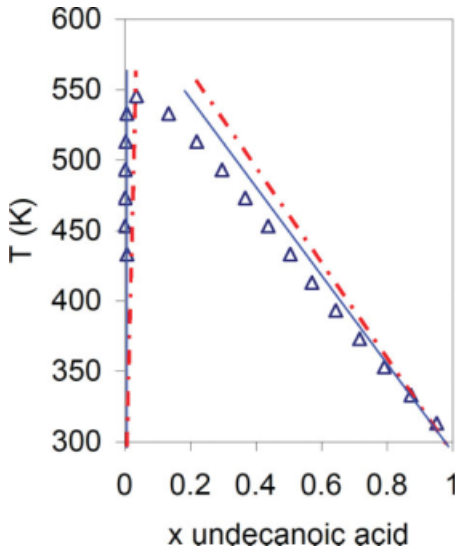

Figure B2. LLE graph for the undecanoic acid + water binary system (k_{ij} = −0.05) using the SPEADMD (solid blue lines) and SPEADCI (dashed red lines).

Experimental data are from Naumova et al.[141] [Color figure can be viewed in the online issue, which is available at www.interscience.wiley.com.]

Manuscript received July 27, 2008, and revision received May 6, 2009.